
Edge of Stochastic Stability: Revisiting the Edge of Stability for SGD

Arseniy Andreyev^{*1} Pierfrancesco Beneventano^{*1}

Abstract

Recent findings by (Cohen et al., 2021) demonstrate that when training neural networks with full-batch gradient descent at a step size of η , the sharpness—defined as the largest eigenvalue of the full batch Hessian—consistently stabilizes at $2/\eta$. These results have significant implications for convergence and generalization. Unfortunately, this was observed not to be the case for mini-batch stochastic gradient descent (SGD), thus limiting the broader applicability of these findings. We show that SGD trains in a different regime we call Edge of Stochastic Stability. In this regime, what hovers at $2/\eta$ is, instead, the average over the batches of the largest eigenvalue of the Hessian of the mini batch (MINIBS) loss—which is always bigger than the sharpness. This implies that the sharpness is generally lower when training with smaller batches or bigger learning rate, providing a basis for the observed implicit regularization effect of SGD towards flatter minima and a number of well established empirical phenomena. Additionally, we quantify the gap between the MINIBS and the sharpness, further characterizing this distinct training regime.

1. Introduction

Training algorithms are a key ingredient to the success of deep learning. Stochastic gradient descent (SGD) (Robbins & Monro, 1951), a stochastic variant of gradient descent (GD), has been effective in finding parameters that yield good test performance despite the complicated nonlinear nature of neural networks.

full-batch GD and its adaptive versions have been shown to optimize in regime of instability (Xing et al., 2018; Jastrzębski et al., 2020; Cohen et al., 2021; 2022). Precisely, if the step size is $\eta > 0$, the highest eigenvalue of the full

batch Hessian, also called full batch sharpness—which we will denote as FULLBS—grows until $2/\eta$ in a first phase of training called progressive sharpening and hovers right above that value, subject to small oscillations. This regime was called Edge of Stability by (Cohen et al., 2021). Surprisingly, unlike for quadratics where it would imply divergence, this instability does not damage convergence when training neural networks.

The work on EOS is about full batch methods. The picture for full batch algorithms seems (empirically) clear, both for GD (Cohen et al., 2021; Damian et al., 2023) and its adaptive and accelerated version (Cohen et al., 2022; 2024). Unfortunately, neural networks are typically trained with the mini-batch versions of these gradient-based methods, and how (Cohen et al., 2021) in Section 6 and Appendices G and H noticed and stated in the introduction and limitations of their work, what they observed is not the case of mini-batch training. Precisely, to quote (Cohen et al., 2021):

[. . .] while the sharpness does not flatline at any value during SGD (as it does during gradient descent), the trajectory of the sharpness is heavily influenced by the step size and batch size (Jastrzębski et al., (Jastrzębski et al., 2019; 2020)), which cannot be explained by existing optimization theory. Indeed, there are indications that the “Edge of Stability” intuition might generalize somehow to SGD, just in a way that does not center around the (full batch) sharpness. [. . .] In extending these findings to SGD, the question arises of how to model “stability” of SGD.

We are the first to our knowledge to define a notion of mini-batch sharpness which acclimates to the learning rate and batch size in a way that reduces to the Edge of Stability in the particular case of full batch algorithms.

What was empirically known for mini-batch SGD. In the case of mini-batch algorithms, (i) (Jastrzębski et al., 2020) noticed that for SGD the phase transition happens earlier for smaller η or smaller batch size b , but they did not quantify when. Moreover, (Cohen et al., 2021) noticed that SGD somehow acclimates to the Hyper parameters. However, they did not characterize how, if not negatively,

^{*}Equal contribution ¹Princeton University, Princeton, NJ, USA. Correspondence to: Arseniy Andreyev <andreyev@princeton.edu>, Pierfrancesco Beneventano <pierb@princeton.edu>.

(ii) it seems not to "flatline" at any value of FULLBS and (iii) if it stabilizes, that always happens at a level they could not quantify which is below the $2/\eta$ threshold, see Figure 1, often without a proper progressive sharpening phase. This scenario leaves the most basic questions open: *In what way the location of convergence of SGD acclimates to the choice of hyperparameters? What are the key quantities involved?* To be more specific, can we characterize the training phenomena in (i), (ii), (iii) above? What determines them? Does SGD train in an unstable regime?

Edge of Stochastic Stability. We address the questions above by introducing a general framework for SGD dynamics through the concept of *Mini-Batch Sharpness* (MINIBS): the average of the highest eigenvalues of the Hessians of mini-batch losses. MINIBS serves as a generalized and direct substitute for full-batch sharpness in SGD settings. Specifically, we identify a new regime, the *Edge of Stochastic Stability* (EOSS), where MINIBS stabilizes near $2/\eta$, while maintaining a critical gap from full-batch sharpness. This dynamic explains the earlier plateau of full-batch sharpness at lower levels determined by batch size, unifying the observed phenomena in mini-batch training.

Moreover, we are able to quantify the level at which FULLBS plateaus during EOSS, by characterizing the gap between MINIBS and FULLBS which empirically typically scales as $(\text{batch size})^{-0.7}$. This needs further investigation, as surprisingly random matrix theory would suggest it scales as $(\text{batch size})^{-1}$.

Organization of the rest of the paper. Section 2 reviews related work and outlines key open questions. In Section 3, we introduce and empirically validate the phenomenon of Edge of Stochastic Stability (EOSS). Section 4 examines values at which Full-Batch Sharpness (FULLBS) plateaus. In Section 5, we discuss the implications for the structure and modeling of SGD dynamics. Finally, Section 6 summarizes our findings and addresses the limitations of this work.

2. Related Work

2.1. Progressive Sharpening and Edge of Stability

Progressive sharpening. Early work noticed that the local shape of the loss landscape changes rapidly at the beginning of the training (LeCun et al., 2012; Keskar et al., 2016; Achille et al., 2017; Jastrzębski et al., 2018; Fort & Ganguli, 2019). Multiple papers noticed growth of different estimators of the FULLBS in the early training (Keskar et al., 2016; Sagun et al., 2016; Fort & Scherlis, 2019; Jastrzębski et al., 2019). Later, (Jastrzębski et al., 2020; Cohen et al., 2021; 2022) managed to make this precise, noticing that along the trajectories of SGD, gradient descent, and full-batch

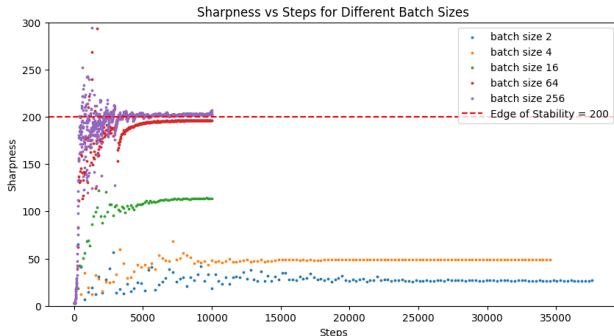


Figure 1. For Mini-batch SGD on CIFAR-10, FULLBS plateaus under the EOS level: the lower the batch size, the lower it plateaus

ADAM the FULLBS usually steadily increases, often after a small number of steps of decrease. This phenomenon, was called progressive sharpening by (Cohen et al., 2021). This is exactly what we reconfirm in our experiments across different models, losses, and datasets. The reason seems to be that in that regime the step size is comparably small and all these gradient-based methods closely follow gradient flow, which steadily increases the FULLBS (Jastrzębski et al., 2020; Cohen et al., 2021), and MINIBS. There is, thus, an empirical agreement on the fact that progressive sharpening is a feature of the loss landscape. To the knowledge of the authors there are no widely accepted explanations of progressive sharpening, we refer the reader to them for further discussion (Li et al., 2022b; Agarwala et al., 2023).

A phase transition. Early studies (Goodfellow et al., 2016; Li et al., 2019; Jiang et al., 2019; Lewkowycz et al., 2020) revealed that large initial learning rates often enhance generalization at the cost of initial loss reduction. (Jastrzębski et al., 2020) attributed this to a sudden phase transition, termed the break-even point, marking the end of progressive sharpening. This transition slows convergence by confining dynamics to a region of lower sharpness. Unlike progressive sharpening, this is considered to be a phenomenon induced by the gradient-based algorithm becoming unstable, not by the landscape. (Jastrzębski et al., 2020; Cohen et al., 2021; 2022) indeed showed that the phase transition comes at different points for different algorithms on the same landscapes. (Jastrzębski et al., 2020) showed that in the case of mini-batch SGD this phase comes earlier for smaller step sizes and smaller batch sizes, without quantifying it. (Cohen et al., 2021) showed indeed that it comes at the instability threshold for the optimization algorithm for full-batch GD and, later (Cohen et al., 2022) for full-batch ADAM.

Full-batch edge of stability. At this points GD and full-batch ADAM transition into an oscillatory regime known as the *Edge of Stability* (EoS) (Cohen et al., 2021), where the FULLBS stabilizes and oscillates around a characteristic

value. The name is due to the fact that, in the case of full-batch GD, the FULLBS hovers at $2/\eta$ which is the stability threshold for optimizing quadratics (Cohen et al., 2021). Observations from (Cohen et al., 2021; 2022) indicate that most training dynamics occur within this regime, effectively defining the FULLBS of the solution. In Appendix A, we explain why the FULLBS in this regime, and MINIBS in the one we describe, is generally above $2/\eta$, rarely aligning exactly. The reasons include: (i) nonlinearity of the loss gradient, which shifts the required value depending on higher-order derivatives, and (ii) the EOS being governed by the Hessian along the gradient direction, rather than FULLBS alone.

EoS and convergence. There is a growing body of work analyzing the surprising mechanism of EOS in training dynamics with GD. Classically, when gradients depend linearly on parameters, divergence occurs locally if $\eta > \frac{2}{\lambda}$, as demonstrated with one-dimensional parabolas (Cohen et al., 2021). Yet, neural networks often converge even when $\eta \geq \frac{2}{\lambda}$, likely due to the problem’s non-standard geometry. (Damian et al., 2023), proposed an explanation under some, empirically tested, assumptions of alignment of third derivatives and gradients. (Wang et al., 2022) showed that the product-like structure of shallow networks guarantees convergence with learning rates exceeding the EOS threshold. For further exploration of convergence and implicit regularization in the EOS regime, we direct readers to (Ahn et al., 2022; Damian et al., 2023; Ahn et al., 2023; Zhu et al., 2023; Lyu et al., 2023).

2.2. SGD, Hessian, and Generalization

SGD finding flatter minima. Our result is inherently a result about mini-batch training improving flatness. Specifically, we explain why *training with smaller batches constrains the dynamics in areas with smaller eigenvalues for the full-batch Hessian*. This quantifies prior observations that SGD tends to locate flat minima (Hochreiter & Schmidhuber, 1994; 1997) and that smaller batch sizes result in reduced Hessian sharpness (Keskar et al., 2016). Analogously, recent work (Jastrzębski et al., 2021) demonstrates that large learning rates in SGD act similarly to penalizing the Fisher matrix’s trace in image classification tasks. As the Fisher matrix approximates the Hessian during training and shares its top eigenspaces (Jastrzębski et al., 2018; Martens, 2020; Thomas et al., 2020), these findings strongly align with our results.

Sharpness and Generalization. SGD-trained networks consistently generalize better than GD-trained ones, with smaller batch sizes further enhancing generalization performance (LeCun et al., 2012; Keskar et al., 2016; Goyal et al., 2017; Jastrzębski et al., 2018; Masters & Luschi, 2018;

Smith et al., 2021). This advantage has been widely attributed to the flatness of the minima (Neyshabur et al., 2017; Wu et al., 2017; Kleinberg et al., 2018; Xie et al., 2020; Jiang et al., 2019; Dinh et al., 2017). Training algorithms explicitly designed to find flat minima, such as (Izmailov et al., 2019; Foret et al., 2021), have indeed demonstrated strong performance across various tasks. Moreover, (Jastrzębski et al., 2021) shows that, in practice, penalizing the trace of the Fisher information matrix empirically improves generalization and reduces memorization—especially when training with noisy labels. We believe that our quantification and the introduction of a theoretical framework for these improvements in sharpness may be a stepping stone towards understanding these generalization benefits theoretically.

3. SGD trains at the Edge of Stochastic Stability

Building on the work of (Cohen et al., 2021), we identify a quantity that stabilizes during training with mini-batch SGD. After introducing the concept of Mini-Batch Sharpness (MINIBS), we empirically establish here the training regime we term the *Edge of Stochastic Stability* across various datasets and architectures. We show not only that MINIBS is a natural quantity to look at but that it is *the correct* natural quantity to describe the training regime.

3.1. Mini-Batch Sharpness

Let $L(\theta, B) := \frac{1}{b} \sum_{(x_i, y_i) \in B} \tilde{L}(f_\theta; x_i, y_i)$ represent the average loss \tilde{L} evaluated on a model f_θ with parameters θ over a batch of data $B = \{(x_i, y_i)\}_{i=1}^b$ of size $b \in \mathbb{N}$. Denote by $\lambda_{\max} [\nabla_\theta^2 L(\theta, B)]$ the largest eigenvalue of the Hessian of the loss $\nabla_\theta^2 L(\theta, B)$ with respect to θ , computed for a given mini-batch B . We now formally define Mini-Batch Sharpness (MINIBS):

Definition 3.1 (Mini-Batch Sharpness (MINIBS)). Let \mathcal{P}_B denote a sampling procedure for mini batches B , we define as Mini-Batch Sharpness the quantity

$$\text{MiniBS} := \mathbb{E}_{B \sim \mathcal{P}_B} [\lambda_{\max} [\nabla_\theta^2 L(\theta, B)]] .$$

MINIBS generalizes the Full-Batch Sharpness (FULLBS)¹:

Definition 3.2 (Full-Batch Sharpness (FULLBS)). Let $\mathcal{D} := \{(x_i, y_i)\}_{i=1}^n$ be a dataset of size $n \in \mathbb{N}$, we denote as Full-Batch Sharpness the quantity

$$\text{FullBS} := \lambda_{\max} [\nabla_\theta^2 L(\theta, \mathcal{D})] .$$

Indeed, when the batch size b approaches the full dataset’s one n , MINIBS reduces to FULLBS. Note that conceptually MINIBS is inherently of the same nature as FULLBS, with

¹Referred to as Sharpness in (Cohen et al., 2021)

Edge of Stochastic Stability

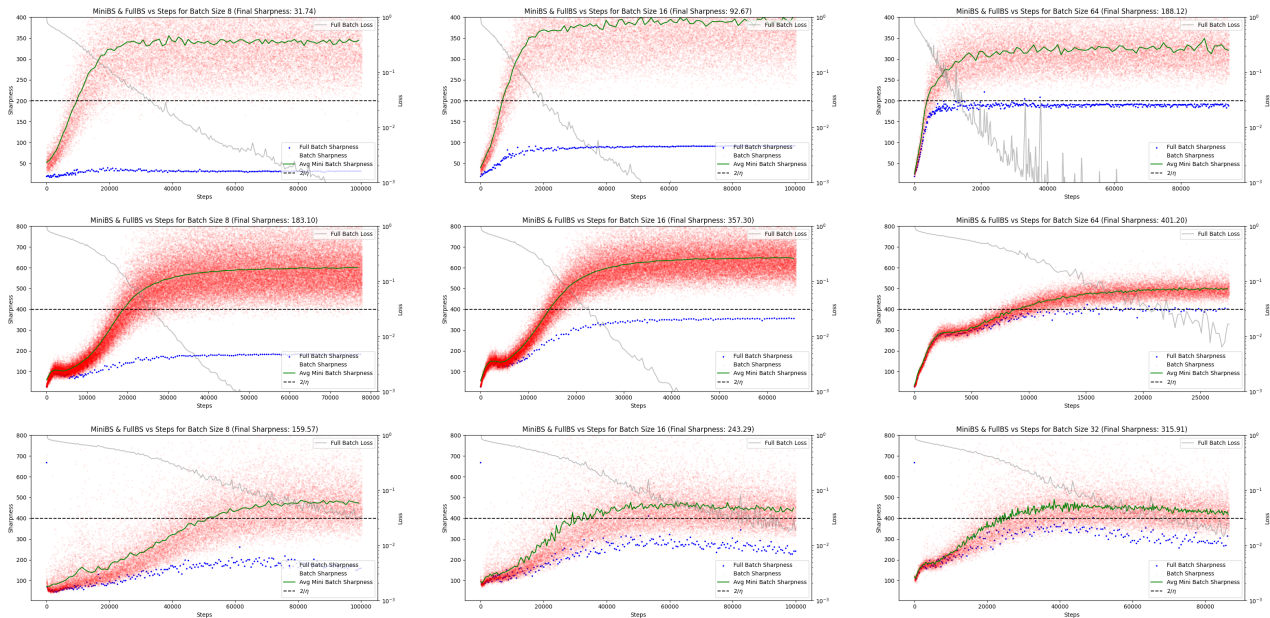


Figure 2. Comparison between: the observed highest eigenvalue for the Hessian of the mini-batch loss (red dots), the empirical MINIBS (green line), the FULLBS (blue dots). *Top*: MLP, 2 hidden layers, hidden dimension 512 *Middle*: CNN, 5 layers *Bottom*: ResNet-14; All trained on a 8k subset of CIFAR-10

the only difference being the "part" of the loss it is computed on—the mini-batch loss for the former, and full-batch loss for the latter. Yet, this difference proves to be crucial in being descriptive of the SGD training dynamics. Indeed, e.g.:

While the mini-batch gradients are an unbiased estimator of the full-batch gradient, the highest eigenvalue of the mini-batch Hessian is not. MINIBS is a positively biased estimator of the FULLBS.

We make this precise in Section 4 where not only we prove that it is biased, we prove that MINIBS is always a strict upper bound to FULLBS in Lemma 4.1, and we quantify it.

3.2. The Edge of Stochastic Stability

We propose that MINIBS serves as *the* generalization of FULLBS in the case of SGD. Precisely, we establish that SGD essentially trains in a regime analogous to Edge of Stability, which we call *Edge of Stochastic Stability* (EOSS), where the MINIBS hovers just above $2/\eta$:

SGD tends to train in an instability regime we call Edge of Stochastic Stability. It is characterized by the fact that after a phase of progressive sharpening, the average MINIBS reaches a stability level of $2/\eta$ or slightly above, and hovers there.

In the EOSS regime, FULLBS also stabilizes, but this is caused by the aforementioned gap between MINIBS and FULLBS. As further discussed in Section 4, EOSS is char-

acterized by the fact that this gap stays constant and depends on the batch size. Consequently, when MINIBS stabilizes, it leads to the stabilization of FULLBS at a level lower than the one of MINIBS by the magnitude of the gap.

3.3. MINIBS is *the* quantity of EOSS

The stabilization of both MINIBS and FULLBS in the EOSS regime raises an important question: why is MINIBS, rather than FULLBS, the quantity that characterizes stabilization in this context?

The primary explanation lies (1) in the relative independence of the MINIBS plateau from the batch size, in contrast to the significant variability observed in the FULLBS plateau. As demonstrated in Figure 2 and supported by additional experiments in Appendix G, the MINIBS plateau consistently lies within a range of $2/\eta$ to at most $2 \times 2/\eta$ across varying batch sizes, models, and learning tasks. In comparison, the FULLBS plateau exhibits fluctuations by an order of magnitude, spanning from $0.1 \times 2/\eta$ to $2/\eta$. This relative stability of MINIBS suggests that it is the quantity that is being stabilized during EOSS. As an even stronger argument, as observed by (Cohen et al., 2021), (2) FULLBS sometimes does not perfectly stabilize, see Figure 2 bottom row in the case of ResNets, while MINIBS always does. When freezing network’s parameters, FULLBS is by definition independent of the batch size, whereas MINIBS varies significantly with the batch size, as further discussed in Section B and illustrated in Figure 9. Therefore, the fact

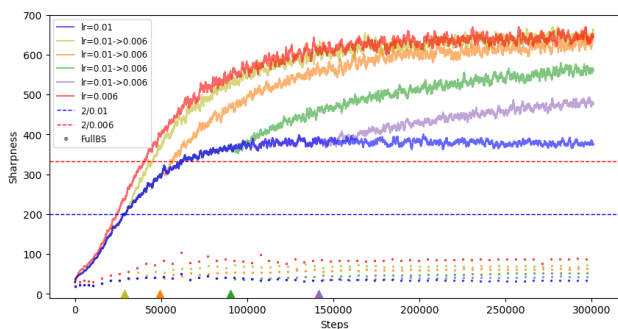


Figure 3. Interaction of MINIBS and FULLBS during EOSS with changes in the LR. The blue and red lines are the dynamics of MINIBS with the LR held constant throughout training. The rest of the colors indicate the dynamics of MINIBS and FULLBS when LR is decreased throughout training. Triangles of corresponding colors indicate the times when the LR was decreased.

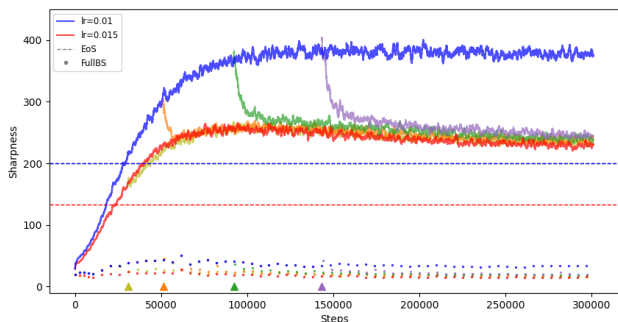


Figure 4. The rest of the colors here indicate the dynamics of MINIBS and FULLBS when LR is increased throughout training. Triangles of corresponding colors indicate the times when the LR was increased.

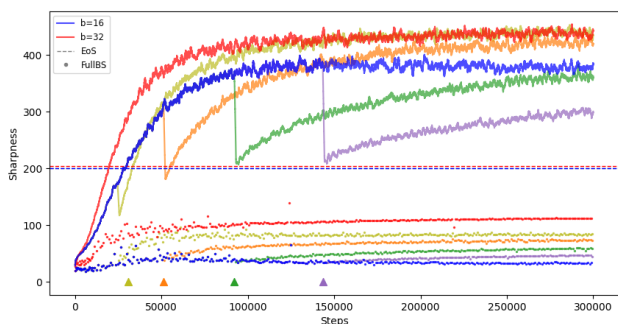


Figure 5. Interaction of MINIBS and FULLBS during EOSS with changes in the batch size. The blue and red lines are the dynamics of MINIBS with the LR held constant throughout training. The rest of the colors indicate the dynamics of MINIBS and FULLBS when batch size is increased throughout training. Triangles of corresponding colors indicate the times when the batch size was increased.

that FULLBS—a quantity that is inherently independent of the batch size—stabilizes at levels that vary significantly with batch size, while MINIBS stabilizes at levels that remain relatively independent of batch size, strongly indicates that MINIBS governs the stabilization process in the EOSS regime. Additionally, there is a theoretical justification for MINIBS being the governing quantity: since gradient updates rely on the loss computed over a batch, the Hessian of this loss (represented by MINIBS) is expected to be the governing quantity of the training process. However, while this explanation aligns with intuition, a rigorous theoretical understanding of the limiting mechanisms underlying the EOS and EOSS regimes is necessary and still missing.

We address in Appendix A the possible reasons why MINIBS plateaus higher than $2/\eta$, exactly as FULLBS at the Edge of Stability under training with full-batch gradient descent (Cohen et al., 2021).

3.4. EOSS is the Natural Generalization of EOS

One of the key characteristics of the EOSS regime is its role as a natural extension of the EOS regime for the case of training under SGD. Specifically, the changes of dynamics of MINIBS with the changes of hyper-parameters mirrors the dynamics of FULLBS, as they are described in as described in (Cohen et al., 2021).

When changing step size. We first demonstrate that in the EOSS regime, MINIBS behaves analogously to FULLBS in the EOS regime when the learning rate (LR) is decreased. As shown in Figure 3, reducing the LR increases the $2/\eta$ threshold, triggering a phase of progressive sharpening. Both MINIBS and FULLBS increase during this phase, eventually stabilizing at new levels. Notably, when training is continued until MINIBS stabilizes, it reaches the same level as a model trained from the start with the reduced LR.

During this phase, the increase in MINIBS allows FULLBS to rise as well, indicating that both quantities undergo progressive sharpening following the LR adjustment. However, while FULLBS stabilizes, it does so at a level lower than that achieved by a network trained entirely with the reduced LR. This divergence from the behavior of FULLBS in full-batch gradient descent warrants further investigation. Despite this, the consistent cycle of progressive sharpening, stabilization, LR adjustment, renewed sharpening, and subsequent stabilization underscores the central role of MINIBS in governing training dynamics.

Another observation that reinforces this argument involves increasing the LR after the network enters the Edge of Stability regime. As shown in Figure 4, increasing the LR effectively lowers the Edge of Stability level, causing both MINIBS and FULLBS to spike significantly before settling at a lower level. Importantly, the new Edge of Stability

level remains much higher than FULLBS. If FULLBS were the "limiting quantity," this adjustment should not impact training dynamics.

However, the observed spike in loss and the subsequent instability until MINIBS stabilizes at its new plateau suggest otherwise. This behavior highlights the role of MINIBS in dictating the training dynamics. For additional clarity, Figure 4 includes a comparison showing a network trained with the larger LR from the beginning.

These observations demonstrate that the interaction between MINIBS and FULLBS during LR changes in the small-batch regime aligns with the analogous sharpness dynamics observed in gradient descent, further solidifying the governing role of MINIBS in the EOSS regime.

When changing batch size. While the behavior described above was already established by (Cohen et al., 2021) in the case of full batch, nothing is known about the training dynamics behavior in case of change of batch size.

To corroborate the discussion above, increasing the batch size reduces the gap between MINIBS and FULLBS, effectively bringing MINIBS closer to FULLBS. Notably, a "jump" in batch size does not alter FULLBS, which remains stable, but significantly impacts the effective MINIBS. This results in a sudden drop in MINIBS, after which both MINIBS and FULLBS begin to increase again, despite being in a plateau phase prior to the jump. This phenomenon also hints to the fact that MINIBS governs the training dynamics. If FULLBS was the quantity of interest, an increase in batch size would not affect it, and the training dynamics would remain unchanged. However, the sudden reduction in MINIBS below the Edge of Stochastic Stability (EOSS) threshold initiates a phase of progressive sharpening—precisely as observed. Once MINIBS stabilizes at its previous level, the progressive sharpening halts, and both MINIBS and FULLBS settle.

Concluding. Our findings confirm and extend the observations of (Cohen et al., 2021) and (Jastrzębski et al., 2020), showing that the highest eigenvalue of the full-batch Hessian (FULLBS) stabilizes below $2/\eta$ for SGD and does so at progressively lower levels for smaller batch sizes. This behavior aligns with empirical results indicating that SGD diverges from the trajectory of small learning rate GD or gradient flow earlier for larger learning rates or smaller batch sizes.

Specifically, we observe that FULLBS stabilizes during training, even with mini batches, and FULLBS for batch size b_1 stabilizes at a value lower than that for batch size b_2 when $b_1 < b_2$, with all other hyperparameters held constant. These results underscore that FULLBS does not serve as a consistent or governing metric for SGD dynamics. Instead,

MINIBS emerges as the critical quantity driving training, especially in the context of small-batch regimes.

4. The size of FULLBS at EOSS: The Gap Decays

In this section, we analyze the size of FULLBS at the Edge of Stochastic Stability and its relationship with MINIBS. We established in Section 3 that MINIBS typically hovers just above $2/\eta$, while FULLBS settles at a much lower value and consistently below $2/\eta$. The exact level at which MINIBS stabilizes is discussed in Appendix A. Here, we focus on estimating the level at which FULLBS levels off, given the stable level of MINIBS.

We establish that:

- MINIBS is always bigger than FULLBS.
- There is no precise rule to describe the value of FULLBS if not through the size of the gap between the two (difference) MINIBS-FULLBS.
- Empirically the gap typically goes as $1/b^\alpha$ generally with $\alpha = 0.70$.
- This is surprising as when fixing the network, the gap goes as $1/b$, i.e., $\alpha = 1$ both empirically and mathematically.

4.1. Ordering the Largest Eigenvalues.

The largest singular value of the Hessian matrix derived from single data points is positive. This observation is crucial in establishing the following well-known property of matrix eigenvalues.

Lemma 4.1. *Let $m, b \in \mathbb{N}$ and consider m matrices $M_1, M_2, \dots, M_b \in \mathbb{R}^{m \times m}$ satisfying $\lambda_{\max} > |\lambda_{\min}|$. Then, the largest eigenvalue of their sum satisfies*

$$\lambda_{\max} \left(\sum_{i=1}^b M_i \right) \leq \sum_{i=1}^b \lambda_{\max}(M_i) \quad (1)$$

with equality only if all M_i are identical.

This lemma is a direct consequence of the convexity of the operator norm in matrices and the fact that the largest eigenvalue is positive in our setting. In our setting, it implies that with non-identical matrices, the maximum eigenvalue of the sum is strictly less than the sum of the maximum eigenvalues of the individual matrices. To illustrate, consider eigenvalue sequences for batch sizes that are powers of four, though the result generalizes to any $b_1 < b_2$:

$$\lambda_{\max}^1 < \lambda_{\max}^4 < \lambda_{\max}^{16} < \lambda_{\max}^{64} < \lambda_{\max}^{256} < \dots \quad (2)$$

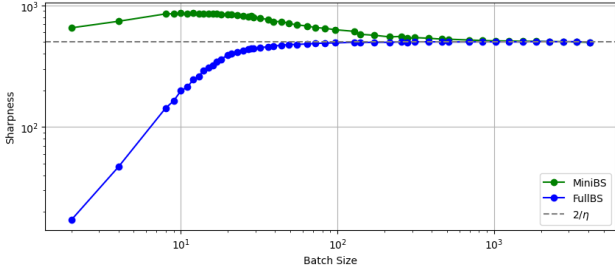


Figure 6. Plot of MINIBS and FULLBS vs batch size at the EOSS.

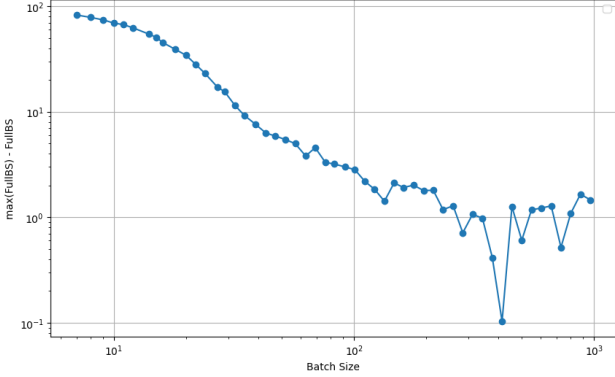


Figure 7. Loglog plot of the gap between the maximum reached by the FULLBS and the FULLBS vs batch size at the EOSS.

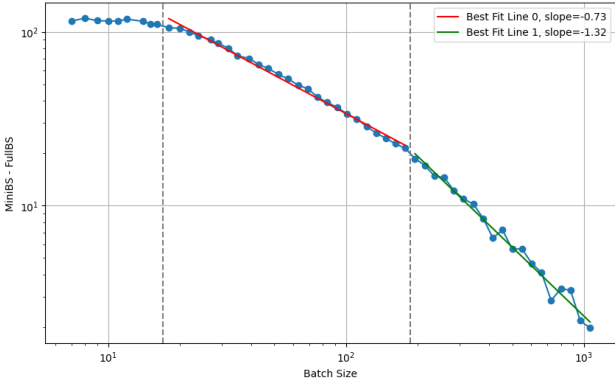


Figure 8. Log-log plot of MINIBS-FULLBS gap vs batch size at the EOSS.

4.2. Empirically Studying the Gap

A natural way to analyze FULLBS across different batch sizes would be to regress FULLBS itself, see Figure 6, or the gap between FULLBS and its maximum value attained, Figure 7. However, these plots often lack a clear structure. What consistently exhibits a clear pattern is the gap between MINIBS and FULLBS. For a fixed batch b we define the gap as:

$$\text{gap} := \text{MiniBS} - \text{FullBS}. \quad (3)$$

Empirically, as shown in Appendix C and Figure 8, the log-log plot of the gap against batch size reveals three distinct regions:

- **Very small b :** for extremely small batch sizes, the gap plateaus. We conjecture that a general lower bound exists for FULLBS, limiting how large the gap can grow. Specifically, the gap is upper-bounded by a quantity of the size $\text{gap} \leq \text{constant}_1/\eta$, otherwise the dynamics exhibits divergence, at the same time FULLBS can not be lower than a certain threshold $\text{FULLBS} \geq \text{constant}_2$. This bound on the gap generally pushes MINIBS higher for these batch sizes, although always in the regime of $\text{constant}_1/\eta$.
- **Typical/moderate b :** the gap consistently scales as $1/b^\alpha$ with approximately $\alpha = 0.7$. This trend dominates for a wide range of practical batch sizes, highlighting the systematic scaling behavior of the MINIBS-FULLBS gap.
- **Very big b :** here generally MINIBS is essentially FULLBS and the gap is converging to zero, we conjecture that some form of scaling limit from random matrix theory applies here. The scaling law is generally of the form: $1/b^\alpha$ with $\alpha \geq 1$. The exact value of α may vary with the setting, but the overall trend is robust.

4.3. Why This is Surprising

While the behavior for very small batches is not surprising, for bigger batch sizes it is. In computer vision tasks where there are way more parameters than datapoints, we observe that the *gap between MINIBS and FULLBS decreases linearly with $1/b$* when evaluating the MINIBS of any fixed model with different batch sizes, see Figure 9.

This scaling is what we expect from our mathematical analysis in Appendix B. We are indeed able to establish that for a fixed net, the gap scales as $1/b$ for small batch sizes, when the worst case MINIBS is very different from FULLBS, and with $1/\sqrt{b}$ for big batch sizes². Indeed:

Proposition 4.2 (Expected Size of the Average of Matrices). *In the notations of Lemma 4.1. Under the same assumptions as Lemma B.1, the spectral norm of the deviation of the average $\|\frac{1}{b} \sum_i M_i - M\|$ from its expectation M satisfies:*

$$\left\| \frac{1}{b} \sum_i M_i - M \right\| = O_b \left(\sqrt{\frac{\sigma^2 \log m}{b}} + \frac{B \log m}{b} \right)$$

where $\sigma^2 = \frac{1}{b} \max\{\|\mathbb{E}[\sum_i M_i^T M_i]\|, \|\mathbb{E}[\sum_i M_i M_i^T]\|\}$ is the expected second moment of the matrices and $B \geq \|M_i - M\|$, for all i , is a bound to the biggest random matrix M_i .

²Although big b means such that the number of directions spanned in the parameter space by the vectors $\nabla_{\theta} f(\theta, x)$ are repeated multiple times, and that may be practically unrealistic with the current sizes of networks.

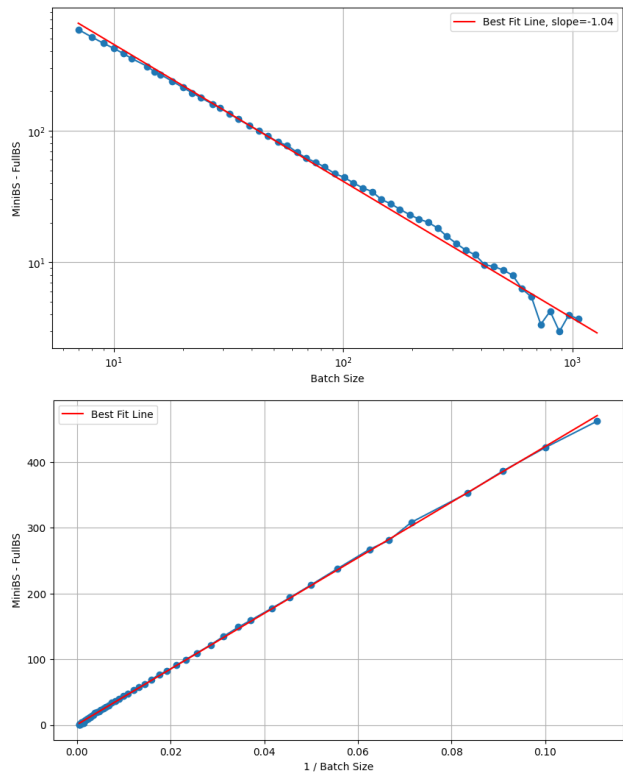


Figure 9. The *static* difference between MiniBS and FullBS vs `batch_size`. The log-log plot is above, indicating the $1/\text{batch_size}$ dependence. The plot with $1/\text{batch_size}$ is below. We fix the parameters of the network at the end of training, and compute the MiniBS using the definition 3.1. This means that the FullBS stays constant, and is subtracted for consistency.

5. Implication: Noise injected full-batch GD \neq mini-batch SGD

5.1. Experiments: SGD vs noisy GD

A prevailing belief in the literature is that SGD’s regularization properties arise from its noisy gradient estimates, which lead to flatter minima. However, our analysis reveals that this effect stems from the *specific directional characteristics* of the noise in SGD.

To investigate this, we compare mini-batch SGD (batch size 16) with three variants of noisy gradient descent (GD):

- *Directional Noise*: GD with noise of Gaussian intensity, but preserving the *directions* and *senses* of the mini-batch noise vectors, as noted in (Simsekli et al., 2019).
- *Diagonal Noise*: GD with Gaussian noise restricted to the diagonal covariance of SGD noise, removing co-directionality while preserving magnitude of the noise.
- *Isotropic Noise*: GD with Gaussian isotropic noise, generating noise vectors of equal magnitude but lacking directional alignment.

Our results (Figure 10) show that **the directions and senses**

of the noise vectors is critical to the dynamics of SGD. This demonstrates that the standard SDE models for SGD, which abstract away directional and orientational noise properties, do not fully capture the dynamics described in this paper.

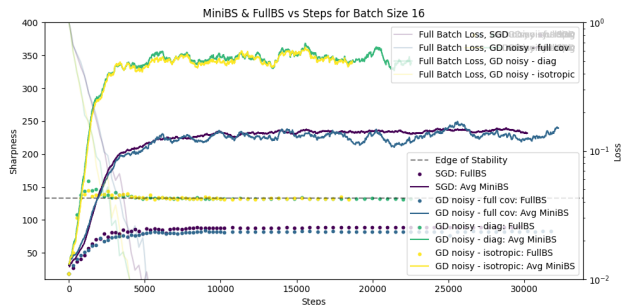


Figure 10. SGD vs Noisy GD. A network only enters the EOSS regime (with the FullBS plateauing well below the $2/\eta$ threshold) when trained with noise that preserves the directionality (aka full covariance) of the SGD noise.

5.2. The Mini-Batch Landscape Matters

Traditional analyses of neural network optimization dynamics adopt two perspectives. (i) *Online Case*: Each sample provides an independent, noisy, unbiased gradient estimate of the theoretical loss, treating SGD as noisy GD on the expected risk. (ii) *Offline Case*: A fixed, finite dataset defines an empirical full-batch loss landscape on which SGD performs noisy optimization. Both views assume a single "real" static landscape through which SGD navigates as a noisy, first-order method. However, our findings emphasize the critical role of the *mini-batch landscape*. An essential insight from our study is, indeed, that the *specific landscape* traversed at each step is crucial, rather than the (either full-batch or expected) static landscape. This distinction becomes evident when considering the variability of mini-batch Hessians, their higher dimensional kernel, and their average sharpness set at $2/\eta$.

5.3. Challenging SDEs as a Model for SGD

Prior probabilistic limitations. The existing literature has already established that SDEs may not adequately model the dynamics of SGD. Notably, (Yaida, 2018) identified that the SDE approximation limits used are often ill-posed, indicating fundamental issues in their application to SGD dynamics. Later, (Li et al., 2021) demonstrated that SDEs do not mimic SGD behaviors except under very specific conditions, such as extremely small learning rates in scale-invariant neural networks where variance dominates the gradient influence. On top of all the above, (HaoChen et al., 2020) showed that various forms of noise—like those from Langevin dynamics or label noise—lead to convergence at

different minima, suggesting diverse dynamics that SDE models may struggle to capture. Finally, (Damian et al., 2021; Li et al., 2022a) have shown that the implicit regularization effects often attributed to diffusion are actually more likely to result from drifts caused by higher-order terms in Taylor expansions. In light of these findings, some recent theoretical efforts have begun to address the discrete nature and account for the different batch-specific Hessians, .e.g., (Roberts, 2021; Smith et al., 2021; Beneventano, 2023), contrasting with much of the earlier literature that does not adequately capture these aspects.

New challenge: geometry of the effective landscape.

Our findings reveal that the dynamics of mini-batch SGD with small batch sizes exhibit significant qualitative differences from those modeled by stochastic optimization trajectories on both full batch and theoretical landscapes. For instance, when employing continuous SDEs on these landscapes, the observed full batch Hessian showcases substantial discrepancies in: (i) The configuration of eigenvectors, as well as the magnitude and quantity of positive eigenvalues compared to those derived from mini-batch processes. (ii) The orientation of these eigenvectors relative to the descent direction, which differs markedly from that observed in mini-batch scenarios. This variation underscores a critical limitation of continuous SDE models in accurately predicting or replicating the nuanced behaviors of mini-batch SGD, particularly when the batch size is small. The inherent differences highlighted by these observations strongly suggest that continuous time models may struggle to provide reliable insights into the pathways and outcomes of mini-batch SGD unless implemented with considerably larger batch sizes.

The problems of continuous-time analysis as highlighted in the prior literature were probabilistic in nature. While advancements in more sophisticated probabilistic tools and distributions, as suggested, e.g., by (Ziyin et al., 2023), may offer potential solutions to them, the challenge of accurately incorporating the variability of batch-specific Hessians into the analyzes remains significant. This complexity underscores a critical gap in our understanding and modeling of SGD dynamics, raising more questions about the feasibility of accurately predicting SGD behavior using existing analyzes.

6. Conclusions, Limitations, and Future Work

Conclusions. This work introduced *Mini-Batch Sharpness* (MINIBS) as a key quantity for understanding and characterizing the dynamics of mini-batch SGD. By showing that MINIBS—rather than the FULLBS—stabilizes at values close to $2/\eta$, we identified a regime we call the *Edge of Stochastic Stability* (EOSS). In EOSS, MINIBS “flat-

lines” near $2/\eta$ while FULLBS hovers below this threshold at a level that systematically depends on the batch size. This complements and generalizes the Edge of Stability (EOS) phenomenon previously documented for full-batch GD (Xing et al., 2018; Cohen et al., 2021; Damian et al., 2023) to the small-batch regime most commonly used in practice.

Our empirical findings reveal that the gap MINIBS – FULLBS decreases as a function of the batch size and generally follows a power law (batch size)^{-0.7} for typical batch sizes across various models and datasets.

Limitations. While our experiments confirm that MINIBS consistently hovers around $2/\eta$ for mini-batch SGD, several limitations remain:

1. **Generalization Beyond Image Classification.** While our experiments focus on image classification tasks, it remains unclear whether the observed dynamics extend to other domains, such as natural language processing or reinforcement learning.
2. **Batch Size Scaling.** Although we empirically identify scaling laws for the MINIBS - FULLBS gap, theoretical justifications, especially for intermediate batch sizes, remain incomplete.
3. **Precision of Hessian-based measurements.** The $\lambda_{\max}(\nabla^2 L)$ can only be estimated through approximation, which presents a specific challenge in quantifying the MINIBS - FULLBS gap, especially when it is significantly smaller than the individual magnitudes.
4. **Scope of hyperparameters and architectures.** Our main experiments focus on constant learning rates and standard architectures. Extensions to other settings, especially large-batch or extremely large-scale models, remain to be systematically explored.
5. **Lack of analysis on momentum and adaptive methods.** While FULLBS “Edge of Stability” phenomena have been observed in ADAM (Cohen et al., 2022), our work does not analytically cover momentum-SGD, ADAM, or other adaptive optimizers in the small-batch regime.

Future Work. On top of working on the limitations, our findings open a number of avenues for further investigation:

- **Deeper theoretical modeling of EOSS.** Extending the self-stabilization arguments of (Damian et al., 2023) and other higher-order analyses (Cohen et al., 2021; Ahn et al., 2022; Lyu et al., 2023) to mini-batch SGD could illuminate precisely why and how MINIBS $\sim 2/\eta$.
- **Batch-size scaling laws.** We observed that the gap MINIBS - FULLBS often follows a power law. A refined analysis could leverage random matrix theory to explain both the “typical” exponent and the potential crossovers for very small or very large batch sizes.

In short, we believe that MINIBS provides a more faithful lens to view and understand the behavior of SGD in modern practice. Our results highlight how mini-batch Hessians fundamentally shape training dynamics in ways that full-batch cannot fully capture. We hope this work spurs further research into small-batch instabilities and sheds new light on how step size and batch size jointly govern the training process in deep networks.

7. Acknowledgement

A special thanks to Stanisław Jastrzębski, Alex Damian, and Boris Hanin for invaluable discussions, which were crucial to the development of this project.

References

- Achille, A., Rovere, M., and Soatto, S. Critical Learning Periods in Deep Neural Networks, 2017. URL <https://arxiv.org/abs/1711.08856v3>.
- Agarwala, A., Pedregosa, F., and Pennington, J. Second-order regression models exhibit progressive sharpening to the edge of stability. In *Proceedings of the 40th International Conference on Machine Learning*, July 2023. URL <https://proceedings.mlr.press/v202/agarwala23b.html>.
- Ahn, K., Zhang, J., and Sra, S. Understanding the unstable convergence of gradient descent. In *Proceedings of the 39th International Conference on Machine Learning*, June 2022. URL <https://proceedings.mlr.press/v162/ahn22a.html>.
- Ahn, K., Bubeck, S., Chewi, S., Lee, Y. T., Suarez, F., and Zhang, Y. Learning threshold neurons via the "edge of stability", October 2023. URL <http://arxiv.org/abs/2212.07469>. arXiv:2212.07469 [cs, math].
- Beneventano, P. On the Trajectories of SGD Without Replacement, December 2023. URL <http://arxiv.org/abs/2312.16143>. arXiv:2312.16143.
- Cohen, J. M., Kaur, S., Li, Y., Kolter, J. Z., and Talwalkar, A. Gradient Descent on Neural Networks Typically Occurs at the Edge of Stability. *arXiv:2103.00065 [cs, stat]*, June 2021. URL <http://arxiv.org/abs/2103.00065>. arXiv: 2103.00065.
- Cohen, J. M., Ghorbani, B., Krishnan, S., Agarwal, N., Medapati, S., Badura, M., Suo, D., Cardoze, D., Nado, Z., Dahl, G. E., and Gilmer, J. Adaptive Gradient Methods at the Edge of Stability, July 2022. URL <http://arxiv.org/abs/2207.14484>. arXiv:2207.14484 [cs].
- Cohen, J. M., Damian, A., Talwalkar, A., Kolter, Z., and Lee, J. D. Understanding Optimization in Deep Learning with Central Flows, October 2024. URL <http://arxiv.org/abs/2410.24206>. arXiv:2410.24206.
- Damian, A., Ma, T., and Lee, J. Label Noise SGD Provably Prefers Flat Global Minimizers. *arXiv:2106.06530 [cs, math, stat]*, June 2021. URL <http://arxiv.org/abs/2106.06530>. arXiv: 2106.06530.
- Damian, A., Nichani, E., and Lee, J. D. Self-Stabilization: The Implicit Bias of Gradient Descent at the Edge of Stability, April 2023. URL <http://arxiv.org/abs/2209.15594>. arXiv:2209.15594 [cs, math, stat].
- Dinh, L., Pascanu, R., Bengio, S., and Bengio, Y. Sharp minima can generalize for deep nets. In *Proceedings of the 34th International Conference on Machine Learning—Volume 70*, pp. 1019–1028. JMLR. org, 2017.
- Foret, P., Kleiner, A., Mobahi, H., and Neyshabur, B. Sharpness-Aware Minimization for Efficiently Improving Generalization, April 2021. URL <http://arxiv.org/abs/2010.01412>. arXiv:2010.01412 [cs, stat].
- Fort, S. and Ganguli, S. Emergent properties of the local geometry of neural loss landscapes, 2019. URL <https://arxiv.org/abs/1910.05929v1>.
- Fort, S. and Scherlis, A. The Goldilocks Zone: Towards Better Understanding of Neural Network Loss Landscapes. *Proceedings of the AAAI Conference on Artificial Intelligence*, 33(01):3574–3581, July 2019. ISSN 2374-3468. doi: 10.1609/aaai.v33i01.33013574. URL <https://ojs.aaai.org/index.php/AAAI/article/view/4237>. Number: 01.
- Goodfellow, I., Bengio, Y., and Courville, A. *Deep learning*. MIT press, 2016.
- Goyal, P., Dollár, P., Girshick, R., Noordhuis, P., Wesolowski, L., Kyrola, A., Tulloch, A., Jia, Y., and He, K. Accurate, large minibatch sgd: Training imagenet in 1 hour. *arXiv preprint arXiv:1706.02677*, 2017.
- HaoChen, J. Z., Wei, C., Lee, J. D., and Ma, T. Shape Matters: Understanding the Implicit Bias of the Noise Covariance. *arXiv:2006.08680 [cs, stat]*, June 2020. URL <http://arxiv.org/abs/2006.08680>. arXiv: 2006.08680.
- Hochreiter, S. and Schmidhuber, J. SIMPLIFYING NEURAL NETS BY DISCOVERING FLAT MINIMA. In *Advances in Neural Information Processing Systems*, volume 7. MIT Press, 1994. URL <https://proceedings.neurips.cc/paper/1994/hash/01882513d5fa7c329e940dda99b12147-Abstract.html>.

- Hochreiter, S. and Schmidhuber, J. Flat minima. *Neural Computation*, 9(1):1–42, 1997. Publisher: MIT Press.
- Izmailov, P., Podoprikin, D., Garipov, T., Vetrov, D., and Wilson, A. G. Averaging Weights Leads to Wider Optima and Better Generalization, February 2019. URL <http://arxiv.org/abs/1803.05407>. arXiv:1803.05407 [cs, stat].
- Jastrzębski, S., Kenton, Z., Arpit, D., Ballas, N., Fischer, A., Bengio, Y., and Storkey, A. Three Factors Influencing Minima in SGD. *arXiv:1711.04623 [cs, stat]*, September 2018. URL <http://arxiv.org/abs/1711.04623>. arXiv: 1711.04623.
- Jastrzębski, S., Kenton, Z., Ballas, N., Fischer, A., Bengio, Y., and Storkey, A. On the relation between the sharpest directions of DNN loss and the SGD step length. 2019.
- Jastrzębski, S., Szymczak, M., Fort, S., Arpit, D., Tabor, J., Cho, K., and Geras, K. The Break-Even Point on Optimization Trajectories of Deep Neural Networks. *arXiv:2002.09572 [cs, stat]*, February 2020. URL <http://arxiv.org/abs/2002.09572>. arXiv: 2002.09572.
- Jastrzębski, S., Arpit, D., Astrand, O., Kerg, G., Wang, H., Xiong, C., Socher, R., Cho, K., and Geras, K. Catastrophic Fisher Explosion: Early Phase Fisher Matrix Impacts Generalization. *arXiv:2012.14193 [cs, stat]*, June 2021. URL <http://arxiv.org/abs/2012.14193>. arXiv: 2012.14193.
- Jiang, Y., Neyshabur, B., Mobahi, H., Krishnan, D., and Bengio, S. Fantastic Generalization Measures and Where to Find Them. *arXiv:1912.02178 [cs, stat]*, December 2019. URL <http://arxiv.org/abs/1912.02178>. arXiv: 1912.02178.
- Keskar, N. S., Mudigere, D., Nocedal, J., Smelyanskiy, M., and Tang, P. T. P. On large-batch training for deep learning: Generalization gap and sharp minima. *arXiv preprint arXiv:1609.04836*, 2016.
- Kleinberg, R., Li, Y., and Yuan, Y. An Alternative View: When Does SGD Escape Local Minima?, August 2018. URL <http://arxiv.org/abs/1802.06175>. arXiv:1802.06175 [cs].
- LeCun, Y. A., Bottou, L., Orr, G. B., and Müller, K.-R. Efficient backprop. In *Neural networks: Tricks of the trade*, pp. 9–48. Springer, 2012.
- Lee, S. and Jang, C. A new characterization of the edge of stability based on a sharpness measure aware of batch gradient distribution. In *International Conference on Learning Representations*, 2023. URL <https://api.semanticscholar.org/CorpusID:259298833>.
- Lewkowycz, A., Bahri, Y., Dyer, E., Sohl-Dickstein, J., and Gur-Ari, G. The large learning rate phase of deep learning: the catapult mechanism. *arXiv:2003.02218 [cs, stat]*, March 2020. URL <http://arxiv.org/abs/2003.02218>. arXiv: 2003.02218.
- Li, Y., Wei, C., and Ma, T. Towards explaining the regularization effect of initial large learning rate in training neural networks. In *Advances in Neural Information Processing Systems*, pp. 11669–11680, 2019.
- Li, Z., Malladi, S., and Arora, S. On the Validity of Modeling SGD with Stochastic Differential Equations (SDEs). *arXiv:2102.12470 [cs, stat]*, June 2021. URL <http://arxiv.org/abs/2102.12470>. arXiv: 2102.12470.
- Li, Z., Wang, T., and Arora, S. What Happens after SGD Reaches Zero Loss? –A Mathematical Framework. *arXiv:2110.06914 [cs, stat]*, February 2022a. URL <http://arxiv.org/abs/2110.06914>. arXiv: 2110.06914.
- Li, Z., Wang, Z., and Li, J. Analyzing Sharpness along GD Trajectory: Progressive Sharpening and Edge of Stability, November 2022b. URL <http://arxiv.org/abs/2207.12678>. arXiv:2207.12678.
- Lyu, K., Li, Z., and Arora, S. Understanding the Generalization Benefit of Normalization Layers: Sharpness Reduction, January 2023. URL <http://arxiv.org/abs/2206.07085>. arXiv:2206.07085 [cs].
- Martens, J. New Insights and Perspectives on the Natural Gradient Method. 2020.
- Masters, D. and Luschi, C. Revisiting Small Batch Training for Deep Neural Networks, April 2018. URL <http://arxiv.org/abs/1804.07612>. arXiv:1804.07612.
- Mishchenko, K., Khaled, A., and Richtarik, P. Random Reshuffling: Simple Analysis with Vast Improvements. In *Advances in Neural Information Processing Systems*, volume 33, pp. 17309–17320. Curran Associates, Inc., 2020. URL <https://proceedings.neurips.cc/paper/2020/hash/c8cc6e90ccbff44c9cee23611711cdc4-Abstract.html>.
- Neyshabur, B., Bhojanapalli, S., Mcallester, D., and Srebro, N. Exploring Generalization in Deep Learning. In Guyon, I., Luxburg, U. V., Bengio, S., Wallach, H., Fergus, R., Vishwanathan, S., and Garnett, R. (eds.), *Advances in Neural Information Processing Systems 30*, pp. 5947–5956. Curran Associates, Inc., 2017. URL <http://papers.nips.cc/paper/7176-exploring-generalization-in-deep-learning.pdf>.

- Robbins, H. and Monro, S. A Stochastic Approximation Method. 1951. URL <https://projecteuclid.org/journals/annals-of-mathematical-statistics/volume-22/issue-3/A-Stochastic-Approximation-Method/10.1214/aoms/1177729586.full>.
- Roberts, D. A. SGD Implicitly Regularizes Generalization Error. *arXiv:2104.04874 [cs, stat]*, April 2021. URL <http://arxiv.org/abs/2104.04874>. arXiv: 2104.04874.
- Sagun, L., Bottou, L., and LeCun, Y. Eigenvalues of the Hessian in Deep Learning: Singularity and Beyond. November 2016. URL <https://openreview.net/forum?id=B186cP9gx>.
- Simsekli, U., Sagun, L., and Gürbüzbalaban, M. A tail-index analysis of stochastic gradient noise in deep neural networks. *CoRR*, abs/1901.06053, 2019. URL <http://arxiv.org/abs/1901.06053>.
- Smith, S. L., Dherin, B., Barrett, D. G. T., and De, S. On the Origin of Implicit Regularization in Stochastic Gradient Descent. *arXiv:2101.12176 [cs, stat]*, January 2021. URL <http://arxiv.org/abs/2101.12176>. arXiv: 2101.12176.
- Thomas, V., Pedregosa, F., Merriënboer, B., Manzagol, P.-A., Bengio, Y., and Roux, N. L. On the interplay between noise and curvature and its effect on optimization and generalization. In *Proceedings of the Twenty Third International Conference on Artificial Intelligence and Statistics*, pp. 3503–3513. PMLR, June 2020. URL <https://proceedings.mlr.press/v108/thomas20a.html>. ISSN: 2640-3498.
- Wang, Y., Chen, M., Zhao, T., and Tao, M. Large learning rate tames homogeneity: Convergence and balancing effect. In *International Conference on Learning Representations*, 2022. URL <https://openreview.net/forum?id=3tbDrs77LJ5>.
- Wu, L., Zhu, Z., and E, W. Towards Understanding Generalization of Deep Learning: Perspective of Loss Landscapes. *arXiv:1706.10239 [cs, stat]*, November 2017. URL <http://arxiv.org/abs/1706.10239>. arXiv: 1706.10239.
- Xie, Z., Sato, I., and Sugiyama, M. A Diffusion Theory For Deep Learning Dynamics: Stochastic Gradient Descent Exponentially Favors Flat Minima. *arXiv:2002.03495 [cs, stat]*, November 2020. URL <http://arxiv.org/abs/2002.03495>. arXiv: 2002.03495.
- Xing, C., Arpit, D., Tsirigotis, C., and Bengio, Y. A Walk with SGD, May 2018. URL <http://arxiv.org/abs/1802.08770>. arXiv:1802.08770 [cs, stat].
- Yaida, S. Fluctuation-dissipation relations for stochastic gradient descent. *arXiv preprint arXiv:1810.00004*, 2018.
- Zhu, X., Wang, Z., Wang, X., Zhou, M., and Ge, R. UNDERSTANDING EDGE-OF-STABILITY TRAINING DYNAMICS WITH A MINIMALIST EXAMPLE. 2023.
- Ziyin, L., Li, H., and Ueda, M. Law of Balance and Stationary Distribution of Stochastic Gradient Descent, August 2023. URL <http://arxiv.org/abs/2308.06671>. arXiv:2308.06671 [cs, stat].

A. Determining the Sharpness of the Plateaus

We try to deduce here at what level the MINIBS plateaus depending on step size η . We highlight three reasons for why the MINIBS sometimes plateaus higher than at $2/\eta$.

A.1. Average MINIBS and effect on FULLBS

FULLBS serves as a strict lower bound for MINIBS values, as further discussed in Section 4 and Appendix B and visible in the point cloud in Figure 2. In particular, depending on the exact mini-batch size, there is often a significant gap between average MINIBS value and FULLBS values, as clear from the plots. Precisely, the smaller the batch size, the bigger the gap between the two, Appendix B. Combined with our conjecture that average MINIBS is plateauing at the EOSS level of slightly above $2/\eta$, this means that the FULLBS is inherently being "forced" to plateau at a level below the EOS. This level is therefore being determined by the gap between the average MINIBS and FULLBS, and is thus determined by the batch size. Precisely, the smaller the batch size, the lower the FULLBS plateau - as confirmed by the FULLBS lines on the Figure 2. This essentially explains the previously unexplained phenomena of why the FULLBS plateaus lower for SGD and is dependent on the batch size.

A.2. Gradient-Hessian Alignment

Mini-batch SGD is exactly gradient descent but on the landscape defined by the mini-batch B . Expanding in Taylor the mini-batch loss $L(\theta, B)$ at a parameter θ after one step of mini-batch SGD performed with learning rate $\eta > 0$ we obtain

$$L(\theta_1, B) = L(\theta_0, B) - \eta \cdot \|\nabla L(\theta_0, B)\|^2 + \frac{\eta^2}{2} \cdot \nabla L(\theta_0, B)^\top \nabla^2 L(\theta_0, B) \nabla L(\theta_0, B) + O(\eta^3) \quad (4)$$

The Edge of Stability, as defined in (Cohen et al., 2021), is the regime in which the last term on the right $\frac{\eta^2}{2} \cdot \nabla L(\theta_0, B)^\top \nabla^2 L(\theta_0, B) \nabla L(\theta_0, B)$ and the term in the middle of the RHS $\eta \cdot \|\nabla L(\theta_0, B)\|^2$ equalize. Training at the Edge of Stability does not mean that the higher eigenvalue of the Hessian is $2/\eta$, means that the quantity

$$\frac{2}{\eta} = \frac{\nabla L(\theta_0, B)^\top \nabla^2 L(\theta_0, B) \nabla L(\theta_0, B)}{\|\nabla L(\theta_0, B)\|^2}. \quad (5)$$

Thus training at the EOS or EOSS is also a question of alignment, not only of size of the highest eigenvalue. Precisely, the highest eigenvalue of the Hessians typically coincides with the operatorial norm of the Hessian and is by definition bigger than the that product. Sometimes, the plateaus is slightly higher than $2/\eta$ for that reason.

A.3. The Model is not Linear

Moreover, when the model is linear and the loss is quadratic, then the loss is a quadratic function and the gradient is a linear function. In this case the EOS and EOSS happen when the Sharpness in Equation 5 is exactly $2/\eta$. Neural networks are not linear models and the thus to impose the LHS of Equation 4 $L(\theta_1, B)$ exactly equal to the value at initialization $L(\theta_0, B)$ it is usually needed to deal with the higher-order terms of the Taylor expansion. As an example, (?) that for shallow linear networks example that we make below in Section ??, the learning rate of the EOS step size is not $\lambda = 2/\eta$ but it is

$$\lambda = \frac{2}{\eta} + \eta \cdot L \pm \eta \sqrt{L}.$$

This may be the reason why we, and before us (Cohen et al., 2021), see that very often the stabilization happens for MINIBS slightly bigger than $2/\eta$.

A.4. Fisher Matrix vs Hessian

In machine learning, the loss L is generally a function of a batch B and the parameterized model f_θ . The Hessian of the loss can thus be decomposed as

$$\frac{1}{b} \sum_{(x_i, y_i) \in B} \underbrace{\nabla_\theta f_\theta(x_i) \cdot \nabla_f^2 L(f, (x_i, y_i)) \cdot \nabla_\theta f_\theta(x_i)^\top}_{\text{Relevant part}} + \underbrace{\nabla_f L(f, (x_i, y_i)) \cdot \nabla_\theta^2 f_\theta(x_i)}_{\text{Converges to zero as } \sqrt{L}} \quad (6)$$

The right summand, when the loss is PL converges to zero together with the loss at the same speed as the square root of it. The left summand instead remains sizeable. For instance, in the case of MSE, the central term $\nabla_f^2 L(f, (x_i, y_i)) = 1$, thus the whole left summand is $\frac{1}{b} \sum_{(x_i, y_i) \in B} \nabla_\theta f_\theta(x_i) \cdot \nabla_\theta f_\theta(x_i)^\top$. This explains how a smaller sharpness at convergence is related to a norm of the smaller Fisher matrix (Jastrzębski et al., 2021). Jastrebsky et al., observed, along this line, how SGD implicitly regularizes the trace of the Fisher matrix (Jastrzębski et al., 2020; 2021),.

The decomposition above in Equation 6 also allows us to study the alignment. Note that for one datapoint and MSE, the Fisher matrix above is

$$\nabla_\theta f_\theta(x_i) \cdot \nabla_\theta f_\theta(x_i)^\top.$$

This is an un-normalized projection matrix along the direction of the gradient of the function $\nabla_\theta f_\theta(x_i)$. Thus it has only one positive eigenvalue $\|\nabla_\theta f_\theta(x_i)\|^2$ with eigenvector the gradient and a kernel of dimension $n - 1$. The gradient of the loss on one datapoint exactly aligns with the top eigenvector, indeed it is

$$\nabla_f L(f, (x_i, y_i)) \cdot \nabla_\theta f_\theta(x_i).$$

This alignment shows why the λ needed to train at EOS/EOSS is generally close to $2/\eta$ and not much bigger. The gradient and the top eigenvalue indeed are the same on one datapoint and anyways have high cosine similarity later.

B. On Largest Eigenvalues of Sums of Matrices

In this section we establish mathematically how the gap between MINIIBS and FULLBS scales with the batch size. Precisely, what size we can expect from the MINIIBS-FULLBS gap for fixed network.

In particular, the following linear algebra results collectively enhance our understanding of the stability and scaling properties of the largest eigenvalues in the context of matrix sums.

B.1. Random Matrix Theory for Scaling Eigenvalues.

While Section 4 establishes mathematically the order of MINIIBS, it lacks of mathematical quantification of their magnitudes. Random matrix theory helps bridging this gap at least for big batch sizes b in the Online SGD case where instead of the full-batch Hessian we take as a reference its theoretical expectation.

Lemma B.1 (Matrix Bernstein Inequality). *Let $n_1, n_2, b \in \mathbb{N}$, let $M_1, M_2, \dots, M_b \in \mathbb{R}^{n_1 \times n_2}$ be independent random matrices satisfying $\mathbb{E}[M_i] = M$ and $\|M_i - M\| \leq B$ for all i , let $v = \max\{\|\mathbb{E}[\sum_i M_i^\top M_i]\|, \|\mathbb{E}[\sum_i M_i M_i^\top]\|\}$ then for all $t > 0$*

$$\mathbb{P}(\|\sum_i M_i - M\| \geq t) \leq (n_1 + n_2) \cdot \exp\left(-\frac{b^2 t^2 / 2}{v + Bbt/3}\right).$$

This lemma provides a probabilistic upper bound on the deviation of the largest eigenvalue as the batch size increases. We now state a proposition that quantifies the expected spectral norm of the average of b matrices M_i based on this inequality.

Proof of 4.2. The Matrix Bernstein inequality bounds the probability of deviation of $|\sum_{i=1}^b (M_i - M)|$ by t . Rescaling by $1/b$, we see that for the average $\overline{M}_b := \frac{1}{b} \sum_{i=1}^b M_i$ we have

$$\mathbb{P}(\|\overline{M}_b - M\| \geq t/b) \leq (n_1 + n_2) \cdot \exp\left(-\frac{b^2 t^2 / 2}{v + Bbt/3}\right).$$

To bound the expectation $\mathbb{E}[\|\overline{M}_b - M\|]$, we use the following general inequality for random variables X with tail bounds:

$$\mathbb{E}[X] \leq \int_0^\infty \mathbb{P}(X \geq t) dt.$$

For $X = \|\overline{M}_b - M\|$, substitute the tail bound:

$$\mathbb{E}[\|\overline{M}_b - M\|] \leq \int_0^\infty (n_1 + n_2) \cdot \exp\left(-\frac{b^2 t^2 / 2}{v + Bbt/3}\right) dt.$$

We now, introduce a substitution to handle the exponential term. Let:

$$z = \frac{b^2 t^2}{v}, \quad \text{so that} \quad t = \sqrt{\frac{vz}{b^2}} \quad \text{and} \quad dt = \frac{1}{2} \sqrt{\frac{v}{b^2 z}} dz.$$

Rewriting the integral in terms of z :

$$\mathbb{E}[\|\bar{M}_b - M\|] \leq (n_1 + n_2) \int_0^\infty \exp\left(-\frac{z}{2 + \frac{Bb}{3\sqrt{\frac{vz}{b^2}}}}\right) \cdot \frac{1}{2} \sqrt{\frac{v}{b^2 z}} dz.$$

While this integral is complex in its full form, we focus on the dominant terms by examining the asymptotics Large b :

- **Variance Contribution:** The v -term dominates when z is small. This leads to a contribution proportional to:

$$O\left(\frac{\sqrt{v \log(n_1 + n_2)}}{b}\right).$$

- **Max Norm Contribution:** The B -term dominates when z is large. This leads to a contribution proportional to:

$$O\left(\frac{B \log(n_1 + n_2)}{b}\right).$$

Combining these contributions gives:

$$\mathbb{E}[\|\bar{M}_b - M\|] = O\left(\frac{\sqrt{v \log(n_1 + n_2)}}{b} + \frac{B \log(n_1 + n_2)}{b}\right).$$

Next note that $v = b \cdot \sigma^2$. This concludes the proof of Proposition 4.2. □

The proposition indicates that as b increases, the expected deviation of \bar{M}_b from M diminishes, with a leading-order term scaling as:

1. **Variance Decay:** The term $\sqrt{\sigma^2/b}$ reflects how the variance contribution decreases as b increases (similar to $1/\sqrt{b}$ scaling for scalar averages).
2. **Norm Bound Decay:** The term B/b reflects how the worst-case individual matrix norm affects the average.
3. **Logarithmic Dimension Dependence:** The $\log(n_1 + n_2)$ factor accounts for the high-dimensional nature of the problem.

C. Dependence of MINIBS-FULLBS gap on the batch size

In this appendix, we further discuss the dependence of the gap between MINIBS and FULLBS from the batch size. As mentioned earlier, there are two distinct cases - the *static* case, and the "trained" case. In the former, we fix a model at some point of the training, and vary the batch size. In particular, FULLBS stays constant, and the only variation comes from MINIBS. In the latter, we fix a batch size at the beginning of the training, and look at the MINIBS-FULLBS gap at the end of the training.

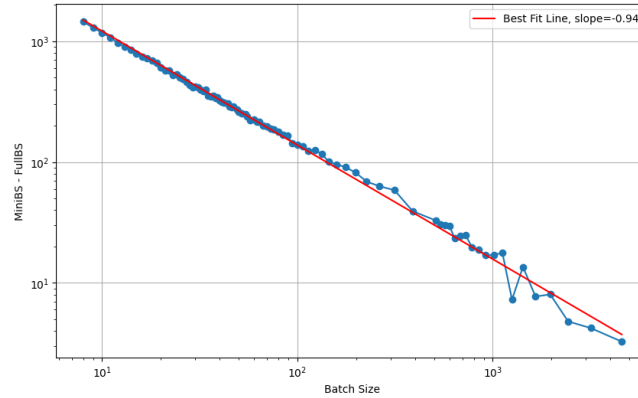


Figure 11. Log-log plot of the MINI-Batch Stochastic Gradient Descent (MINIBS)-Full Batch Stochastic Gradient Descent (FULLBS) for fixed model at convergence.

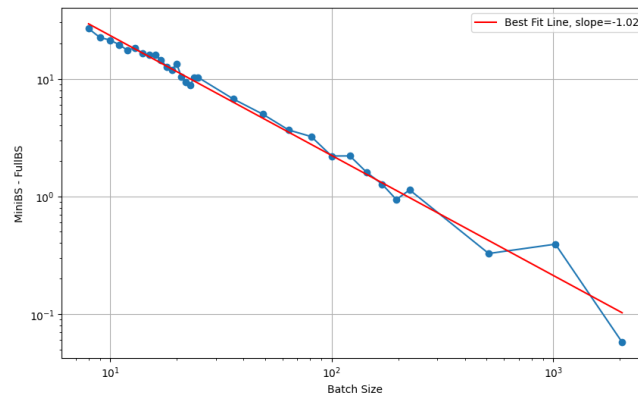


Figure 12. Log-log plot of the MINI-Batch Stochastic Gradient Descent (MINIBS)-Full Batch Stochastic Gradient Descent (FULLBS) for a model at initialization

C.1. The static case

For the *static* case, we first look at a network at the end of training. The network is a perceptron with two hidden layers of dimension 512, trained with batch size of 256 on a 8k subset of CIFAR-10 to convergence. Log-log plot in Figure 11 confirms an approximate $1/\text{batch_size}$ dependence.

One can notice that at high batch sizes the observed slope is somewhat bigger (-1.1 if fitted to the MINI-Batch Stochastic Gradient Descent (MINIBS)-Full Batch Stochastic Gradient Descent (FULLBS) computed for batch sizes larger than 1000). Now, for a dataset of size 8k, a batch size of 1000 constitutes $1/8$ of dataset, and thus has the MINI-Batch Stochastic Gradient Descent (MINIBS) very close to the Full Batch Stochastic Gradient Descent (FULLBS). This might potentially reveal a different scaling regime for batch sizes that are closer to dataset size. On the other hand, since the difference between MINI-Batch Stochastic Gradient Descent (MINIBS) and Full Batch Stochastic Gradient Descent (FULLBS) becomes increasingly small when batch size approaches dataset size (especially in comparison to the value of each: MINI-Batch Stochastic Gradient Descent (MINIBS)-Full Batch Stochastic Gradient Descent (FULLBS) being of order of 1, and each being around 500), the change in scaling might just be an effect of noise in estimating the highest eigenvalue of the hessian. Lastly, there is the effect of finiteness of the dataset size - that is, that the $1/b$ dependence would turn to 0 only when b is infinite, although in reality the gap would be 0 when b is equal to the dataset size. This dependence might effectively break the scaling. Answering the above questions necessitates further investigation. Nonetheless, the $1/b$ dependence appears to persist within the 'realistic' SGD regime, characterized by batch sizes that are substantially smaller than the dataset size.

The $1/b$ scaling appears to hold throughout the training. In particular, it also applies at initialization, as showcased in the log-log in Figure 12.

Moreover, the $1/b$ dependence is also architecture-independent. As illustrated in the log-log plot in Figure 13, it is also the case for a CNN architecture at convergence.

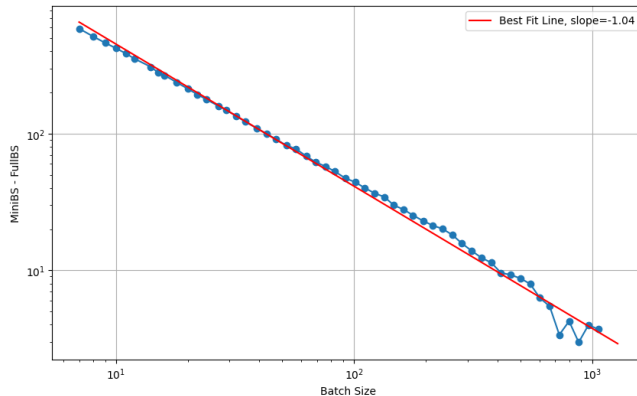


Figure 13. Log-log plot of the MINI-Batch Stochastic Stability (MINIBS) minus Full-Batch Stochastic Stability (FULLBS) for *fixed* CNN model at convergence.

C.2. The trained case

As illustrated in Figure 14, the $1/\text{batch_size}$ dependence breaks down in the trained case, holding only within specific ranges of batch sizes. Specifically, for batch sizes in the range $[10, 100]$ the gap appears to scale as $1/b^{0.7}$. Meanwhile, for batch sizes in $[100, 1000]$, the gap scales as $1/b$. The corresponding regimes are depicted in Figure 15 and in Figure 16.

Similar to the static case, we again see that the anomalous region at batch sizes that are larger than $1/8$, requiring further investigation. A distinct scaling regime emerges for very small batch sizes (< 10), differing from the patterns described above. In this regime, the gap appears largely independent of the batch size. This anomaly might arise because, at such small batch sizes, the MINI-Batch Stochastic Stability (MINIBS) starts at levels at or beyond the Edge of Stochastic Stability (EOSS) level, bypassing the standard progressive sharpening phase and instead entering a regime where the Full-Batch Stochastic Stability (FULLBS) decreases. Further investigation is necessary to rigorously characterize the scaling behavior in this regime.

D. The Hessian and the Fisher Information Matrix Overlap

We show here empirically that at EOSS generally MINI-Batch Stochastic Stability (MINIBS) generally overlaps with the largest eigenvalue of the averaged mini-batch NTK and $\frac{1}{b} J_B^\top J_B$, which corresponds with the Fisher Information Matrix (FIM) in vision classification tasks. See Figure 17.

E. On the Redefinitions of EOS for mini-batch SGD

The question on how to redefine EOS phase for the mini-batch case is not obvious. The defining features of the full-batch notion of Edge of Stability are that

1. There exists a phase in which FULLBS is stable and present oscillations around the instability threshold.
2. The steps are such that the second and third order terms of the Taylor expansion of the loss $L(\theta)$ evolution cancel out. Indeed, θ_1 after one step of full-batch GD with step size $\eta > 0$ from θ_0 is such that

$$L(\theta_1) = L(\theta_0) + \eta \cdot \|\nabla L(\theta_0)\| - \underbrace{\frac{\eta^2}{2} \cdot \nabla L(\theta_0)^\top \nabla^2 L(\theta_0) \nabla L(\theta_0)}_{\text{cancel out at the Edge of Stability}} + O(\eta^3). \quad (7)$$

3. The FULLBS during this phase implicitly defines the sharpness of the minimum found by gradient descent.
4. This phenomenon is unexpected in the understood cases of optimization of quadratics.

Mini batch SGD with fixed step size is known to oscillate because of its inherent noise even in the case of quadratics at convergence. Precisely, at convergence, it oscillate around a minimum with size of the oscillations η for the case with replacement or η^2 for the case without replacement, see (Mishchenko et al., 2020) and references therein. SGD thus exhibits the properties 1. and 3. naturally, even for quadratics, not because of an instability due to the landscape, but because of an instability due to the noise. The only previous work connecting EOS and SGD present to our knowledge describe an effect

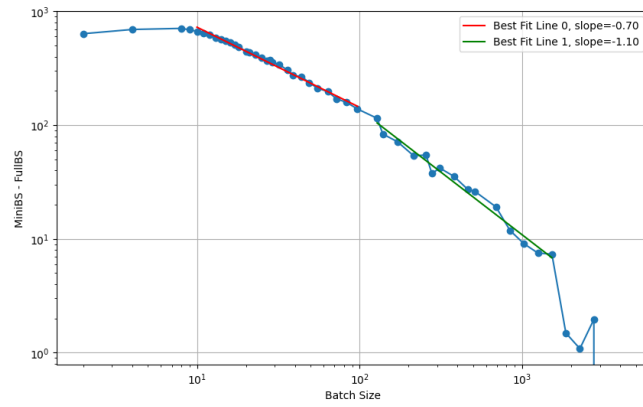


Figure 14. Log-log plot of MINI-B-S-FULL-B-S gap vs batch size at the EOSS. Notice how the scaling breaks for very small and very large batch sizes

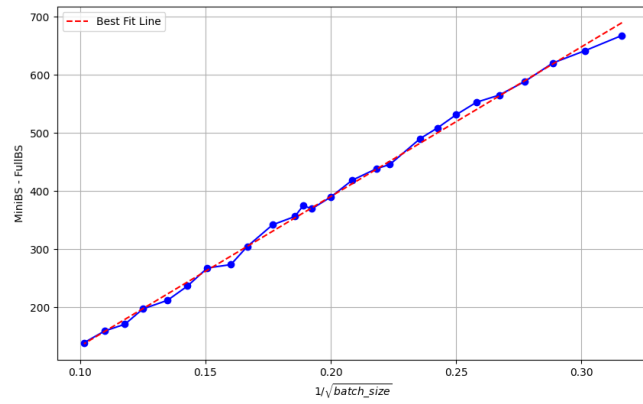


Figure 15. MINI-B-S-FULL-B-S gap vs $1/\sqrt{\text{batch_size}}$ at the EOSS, for batch sizes in $[10, 100]$.

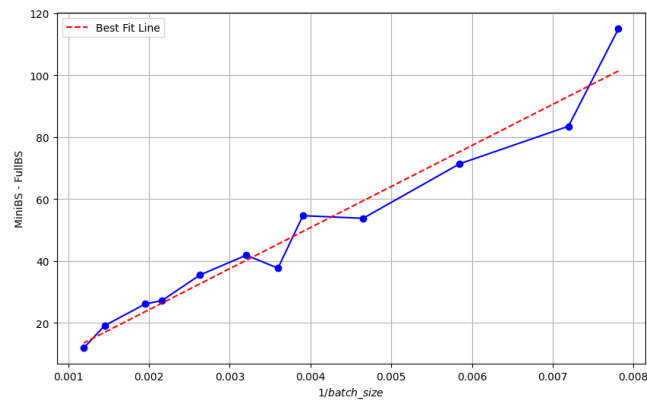


Figure 16. MINI-B-S-FULL-B-S gap vs $1/\text{batch_size}$ at the EOSS, for batch sizes in $[100, 1000]$.

Edge of Stochastic Stability

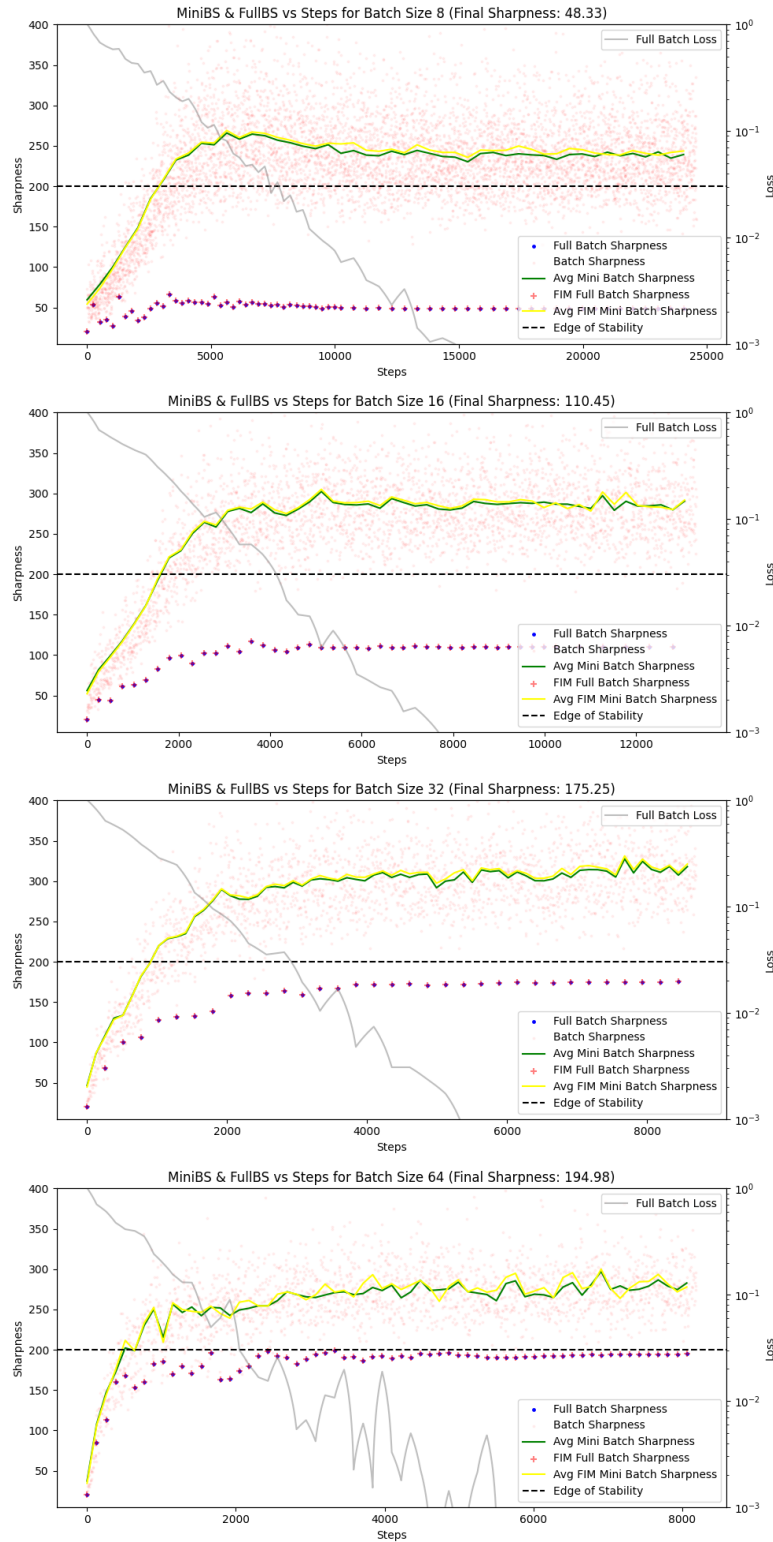


Figure 17. Ranging different batch sizes, the MINIBS corresponds to the largest eigenvalue of the averaged mini-batch NTK and $\frac{1}{b} J_B^T J_B$, which corresponds with the FIM in vision classification tasks.

which contains this natural effect due to SGD noise. The effect we discover and the generalization to mini batches that we give for edge of stability instead is about an instability due to the landscape, and thus about the properties **2.** and **4.** above. Edge of stability is about having a quantity that is around $2/\eta$; it is also about the canceling out in the equation above, but it is not only about the oscillations per se. We thus believe that this is the generalization of Edge of Stability for the mini-batch setting that is interesting for understanding the training dynamics of deep learning and that naturally generalizes the one given by (Cohen et al., 2021) for full-batch GD and by (Cohen et al., 2022) for full-batch ADAM. Indeed, EOSS reduces to EOS in the full batch case and our empirical observations are inherently of how our relevant notion of sharpness acclimates to learning rate and batch size. The only other work on extending the EOS for mini-batch SGD is (Lee & Jang, 2023), but there the authors are rather presenting a non-consistent correction term to the GD EOS to get the EOS for SGD, without establishing its limiting factor or the influence on the dynamics of SGD.

F. Exemplification Through a Simplified Model

To elucidate what the size of the MINIBS, consider a simplified scenario involving a diagonal linear network trained on data from two orthogonal classes. Assume $(x, y) \in \mathbb{R}^2 \times \mathbb{R}$ is either $z_1 = ((1, 0), 1)$ or $z_2 = ((0, 1), -1)$ with probability $1/2$. We learn this data with a diagonal linear network and MSE, precisely where

$$f(x) = a^\top B \cdot x, \quad a \in \mathbb{R}^2, \quad B \in \mathbb{R}^{2 \times 2}.$$

Then with a diagonal initialization, gradient descent will converge almost surely to a neural network of the following kind

$$f(x) = (a_1, a_2) \cdot \begin{pmatrix} b_1 & 0 \\ 0 & b_2 \end{pmatrix} \cdot x, \quad \text{where } |a_1 \cdot b_1| = |a_2 \cdot b_2| = 1.$$

At convergence, the spectrum of the Hessian on the data point z_1 is $\{\lambda_1, 0, 0, 0, 0, 0\}$, with $\lambda_1 := a_1^2 + b_1^2$, the Hessian on the data point z_2 is instead $\{\lambda_2, 0, 0, 0, 0, 0\}$, where $\lambda_2 := a_2^2 + b_2^2$, and the two eigenvectors for these two eigenvalues are orthogonal between each other. This implies that the Hessian of the full batch loss has spectrum $\{\lambda_1/2, \lambda_2/2, 0, 0, 0, 0\}$, while the Hessian on the mini batches of size one has either one of the spectra above.

This implies that

$$\text{FullBS} = \lambda_{\max} \left(\frac{1}{2} \mathcal{H}(z_1) + \frac{1}{2} \mathcal{H}(z_2) \right) = \max \left\{ \frac{\lambda_1}{2}, \frac{\lambda_2}{2} \right\} \quad (8)$$

This is smaller than the average largest eigenvalue of the mini-batch Hessian which is

$$\text{MiniBS} = \frac{1}{2} \lambda_{\max}(\mathcal{H}(z_1)) + \frac{1}{2} \lambda_{\max}(\mathcal{H}(z_2)) = \frac{\lambda_1}{2} + \frac{\lambda_2}{2}. \quad (9)$$

- **Smaller size:** Thus setting $FullBS$ equal to λ means that the max between λ_1 and λ_2 is exactly 2λ . Note that the fact that $a_1 \cdot b_1 = a_2 \cdot b_2 = 1$ and Cauchy-Schwartz imply that $\lambda_1, \lambda_2 \geq 2$. Setting $MiniBS$ to λ thus implies that the maximum between λ_1 and λ_2 is *at most* $2\lambda - 2$, generally smaller.
- **Higher alignment:** Moreover, we have that the gradient $\nabla f(z_i)$ on the data point z_i exactly aligns with the eigenvector v_i of the highest eigenvalue λ_i of the Hessian in z_i . On the full batch, we are averaging them differently, precisely we have that there exist two constants c_1, c_2 such that the gradient is $\frac{c_1}{2} v_1 + \frac{c_2}{2} v_2$. Thus, where WLOG $\lambda_1 > \lambda_2$ we have the alignments

$$\mathcal{H}(z_1) \cdot \nabla L(z_1) \sim c_1 \lambda_1^2 v_1 \quad \text{but} \quad \mathcal{H} \cdot \nabla f \sim \frac{c_1}{2} \lambda_1^2 v_1 \quad (10)$$

Thus one half of it (batch size divided by number of data points).

This shows that in the same point of the gradient, SGD perceives the largest eigenvalue of the Hessian bigger and more relevant to the gradient than GD.

G. Illustration of EOSS in Variety of Settings

In this appendix, we provide further empirical evidence that EOSS arises robustly across a variety of models, step sizes, and batch sizes. Consistent with our main observations, we find that MINIBS invariably stabilizes within the interval $[2/\eta, 2 \times 2/\eta]$, while FULLBS remains strictly below MINIBS, with a gap that widens as the batch size decreases.

MLP (2-Layer) Baseline. Figure 18 illustrates EOSS for our baseline network, an MLP with two hidden layers of dimension 512, trained on an 8192-sample subset of CIFAR-10 with step size $\eta = 0.004$. As the training proceeds, MINIBS stabilizes in the range $[2/\eta, 2 \times 2/\eta]$, whereas FULLBS plateaus strictly below MINIBS. Decreasing the step size to $\eta = 0.002$ (see Figure 19) rescales the plateau of MINIBS around the new threshold $2/\eta$, in line with the behavior discussed in the main text.

Deeper MLP (4-Layer). To assess whether increased depth alters the phenomenon, we use a deeper MLP (MLP_L) with four hidden layers, training again on the same CIFAR-10 subset. Figures 20 and 21 show that MINIBS exhibits the same EOSS behavior for two different step sizes, reinforcing that depth alone does not invalidate our findings.

5-Layer CNN. We further confirm the EOSS regime in a five-layer CNN. As depicted in Figures 22 and 23, MINIBS continues to plateau near the instability threshold for two distinct step sizes, while FULLBS once again settles at a lower level. Notably, as we vary the batch size, the gap between MINIBS and FULLBS increases for smaller batches, mirroring the patterns described in Section 4.

ResNet-10. Finally, we demonstrate that the EOSS regime also emerges for a canonical architecture commonly used in computer vision: RESNET-10. Figure 24 highlights the same qualitative behavior, with MINIBS stabilizing at $[2/\eta, 2 \times 2/\eta]$ and FULLBS remaining consistently below MINIBS.

Overall, these experiments provide further confirmation that EOSS is a robust phenomenon across different architectures, step sizes, and batch sizes. Although the specific magnitude of FULLBS and the exact “hovering” value of MINIBS can vary, the overarching pattern of $\text{MINIBS} \approx 2/\eta$ and $\text{FULLBS} < \text{MINIBS}$ persists in all our tested settings.

Edge of Stochastic Stability

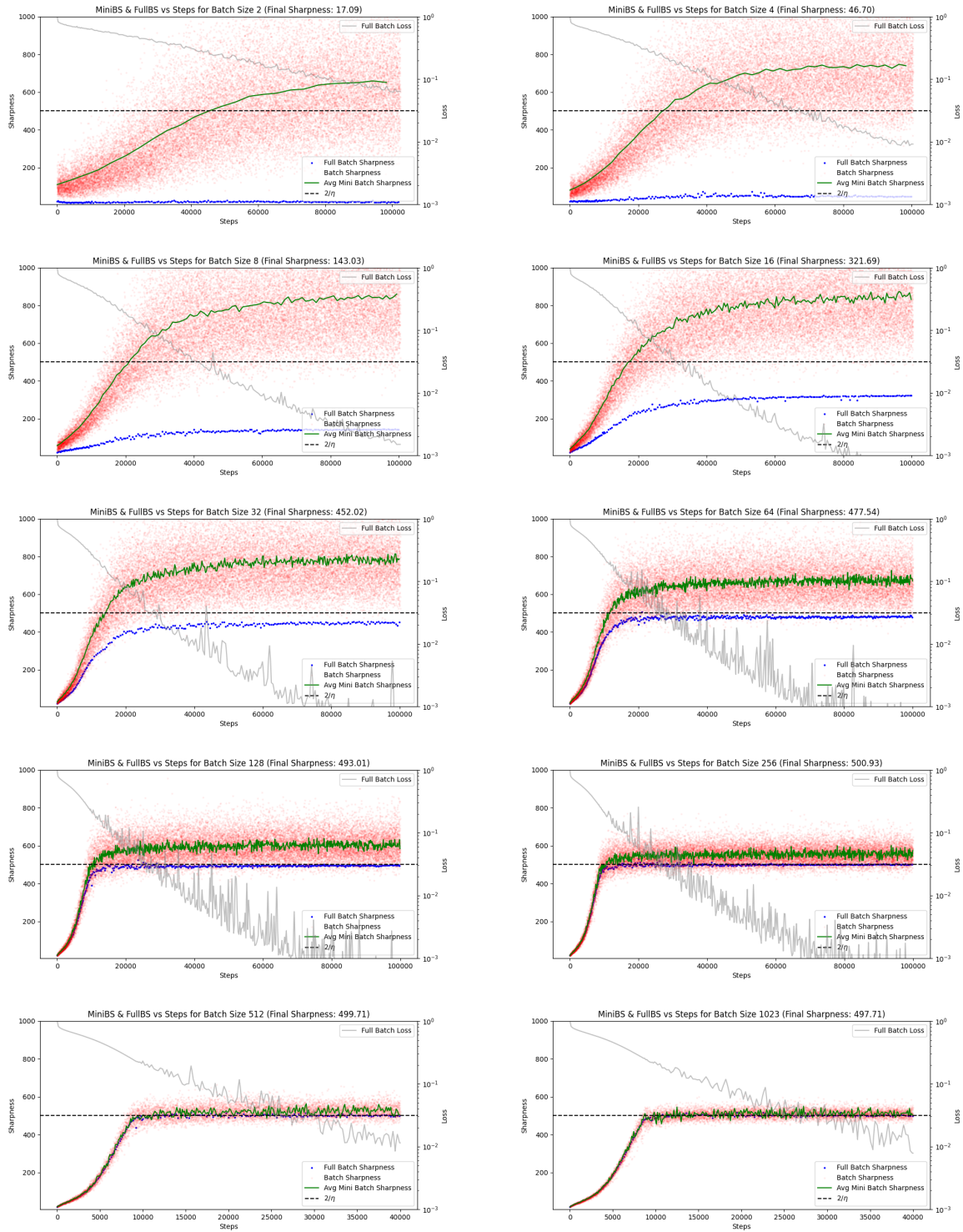


Figure 18. MLP, 2 hidden layers, hidden dimension 512, LR 0.004, 8k subset of CIFAR-10. Comparison between: the observed highest eigenvalue for the Hessian of the mini-batch loss (red dots), the empirical MINIBS (green line), the FULLBS (blue dots).

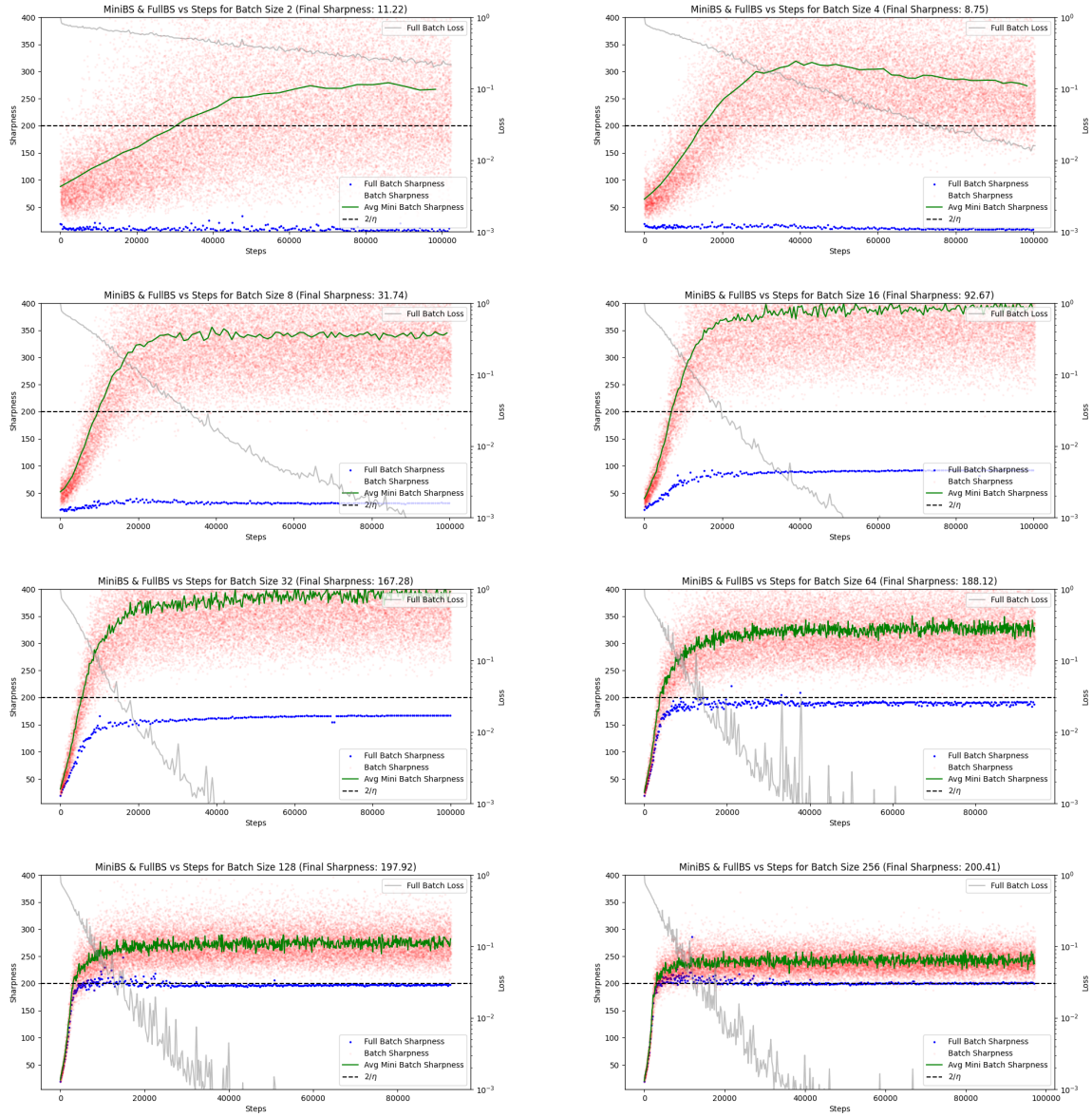


Figure 19. MLP: 2 hidden layers, hidden dimension 512; LR 0.01, 8k subset of CIFAR-10. Comparison between: the observed highest eigenvalue for the Hessian of the mini-batch loss (red dots), the empirical MINIBS (green line), the FULLBS (blue dots).

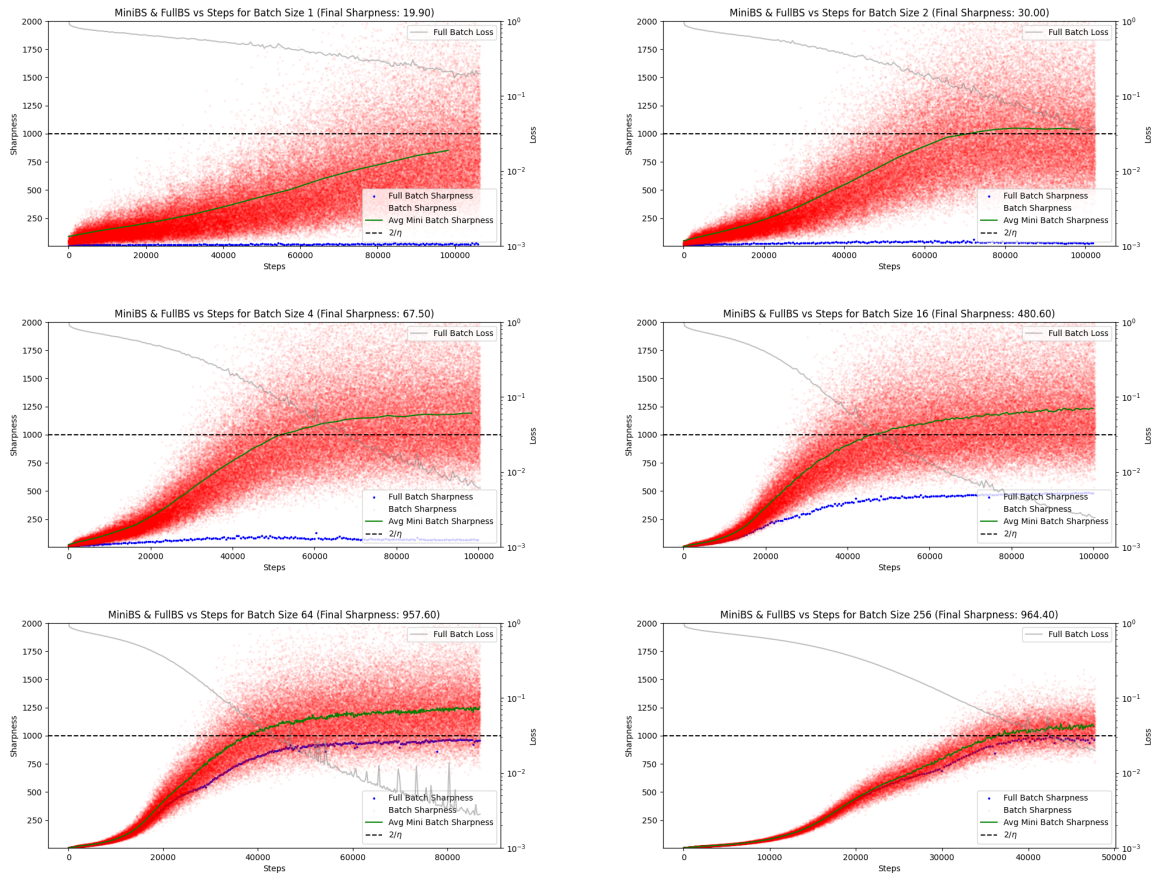


Figure 20. MLP_L: **4 hidden layers**, hidden dimension 512, **LR 0.002**, 8k subset of CIFAR-10. Comparison between: the observed highest eigenvalue for the Hessian of the mini-batch loss (red dots), the empirical MINIBS (green line), the FULLBS (blue dots).

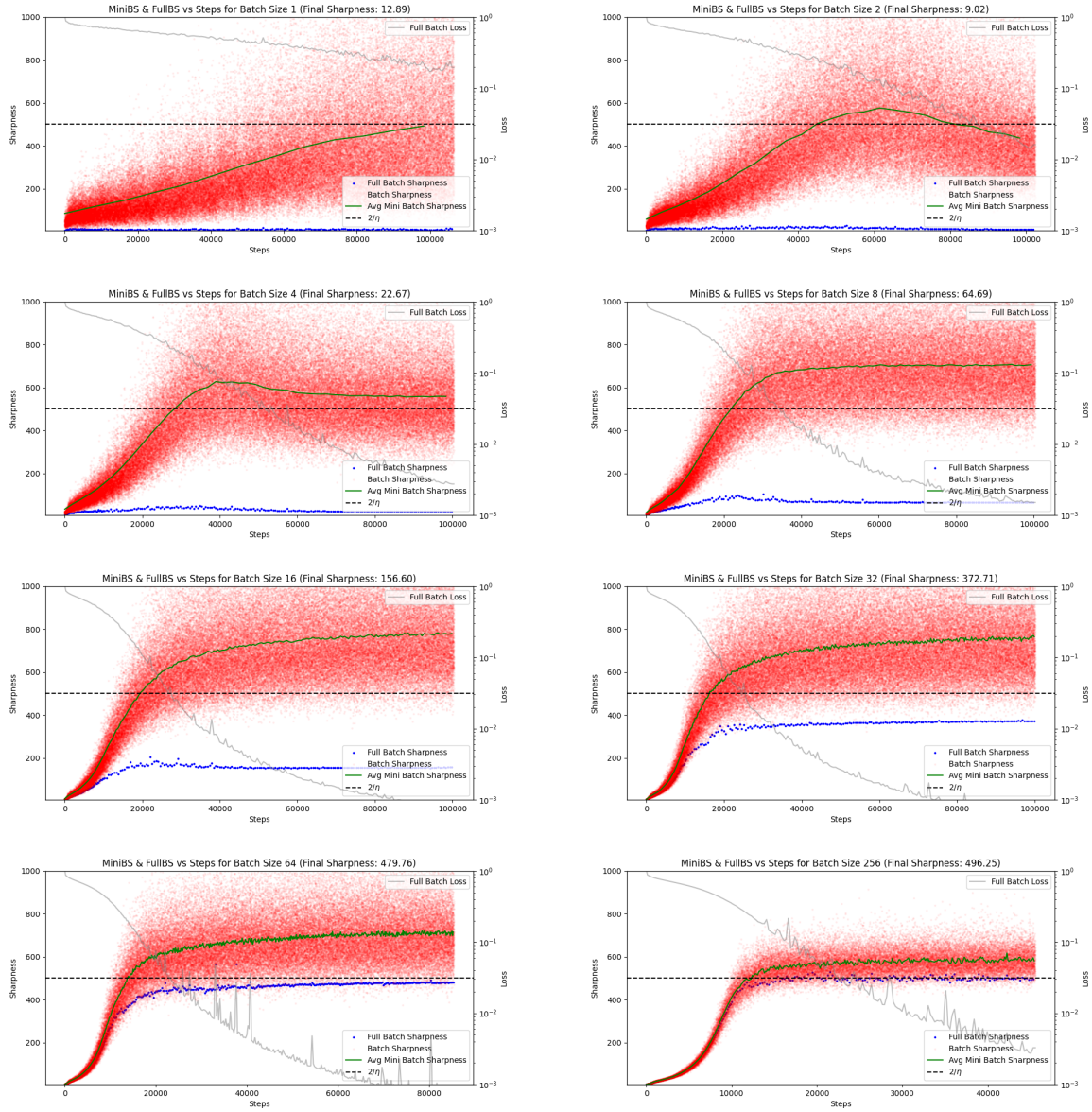


Figure 21. MLP_L, 4 hidden layers, hidden dimension 512, LR 0.004, 8k subset of CIFAR-10. Comparison between: the observed highest eigenvalue for the Hessian of the mini-batch loss (red dots), the empirical MiniBS (green line), the FullBS (blue dots).

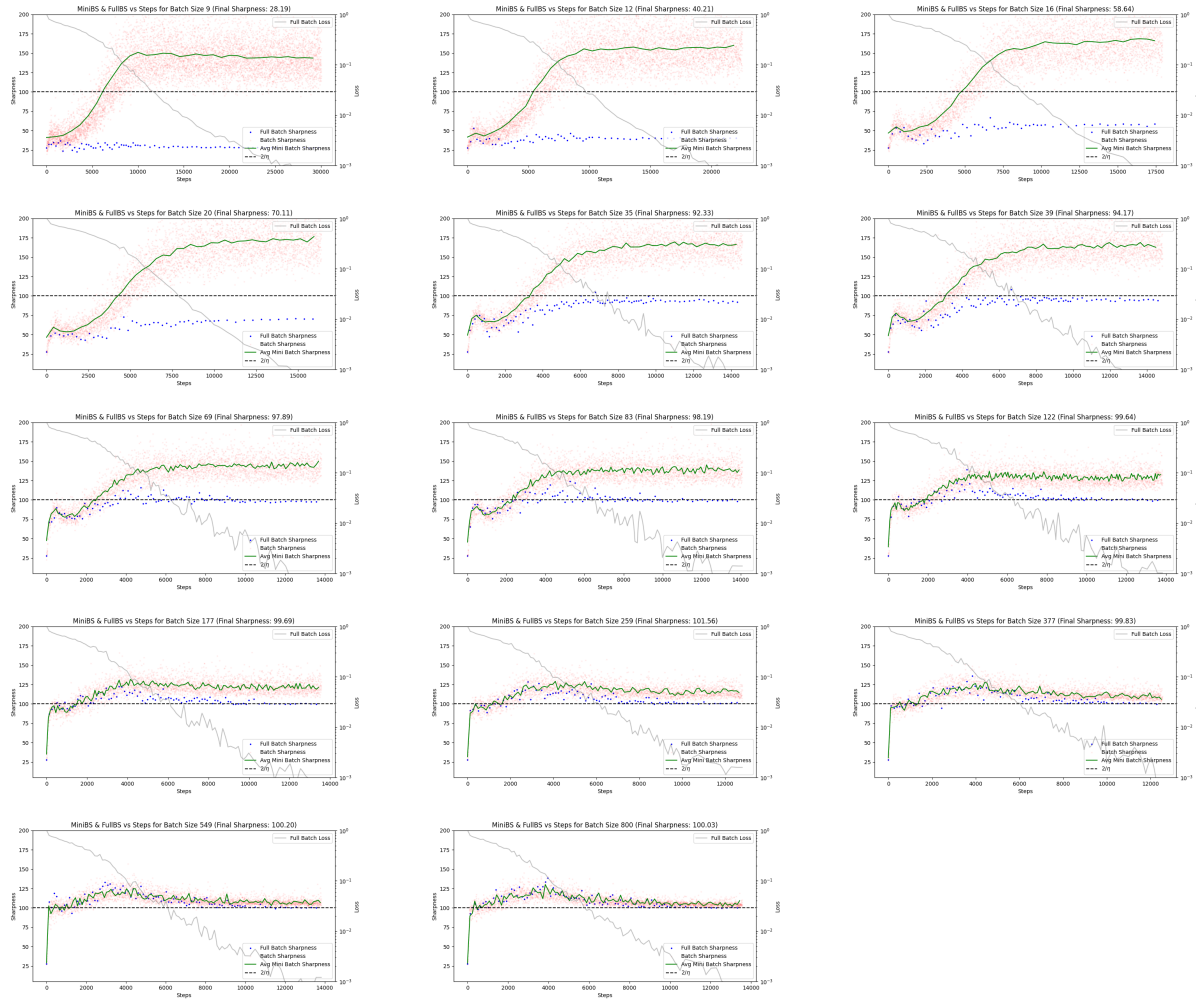


Figure 22. CNN, 4 layers (3 convolutional, 2 fully-connected), LR 0.02, 8k subset of CIFAR-10. Comparison between: the observed highest eigenvalue for the Hessian of the mini-batch loss (red dots), the empirical MINIBS (green line), the FULLBS (blue dots).

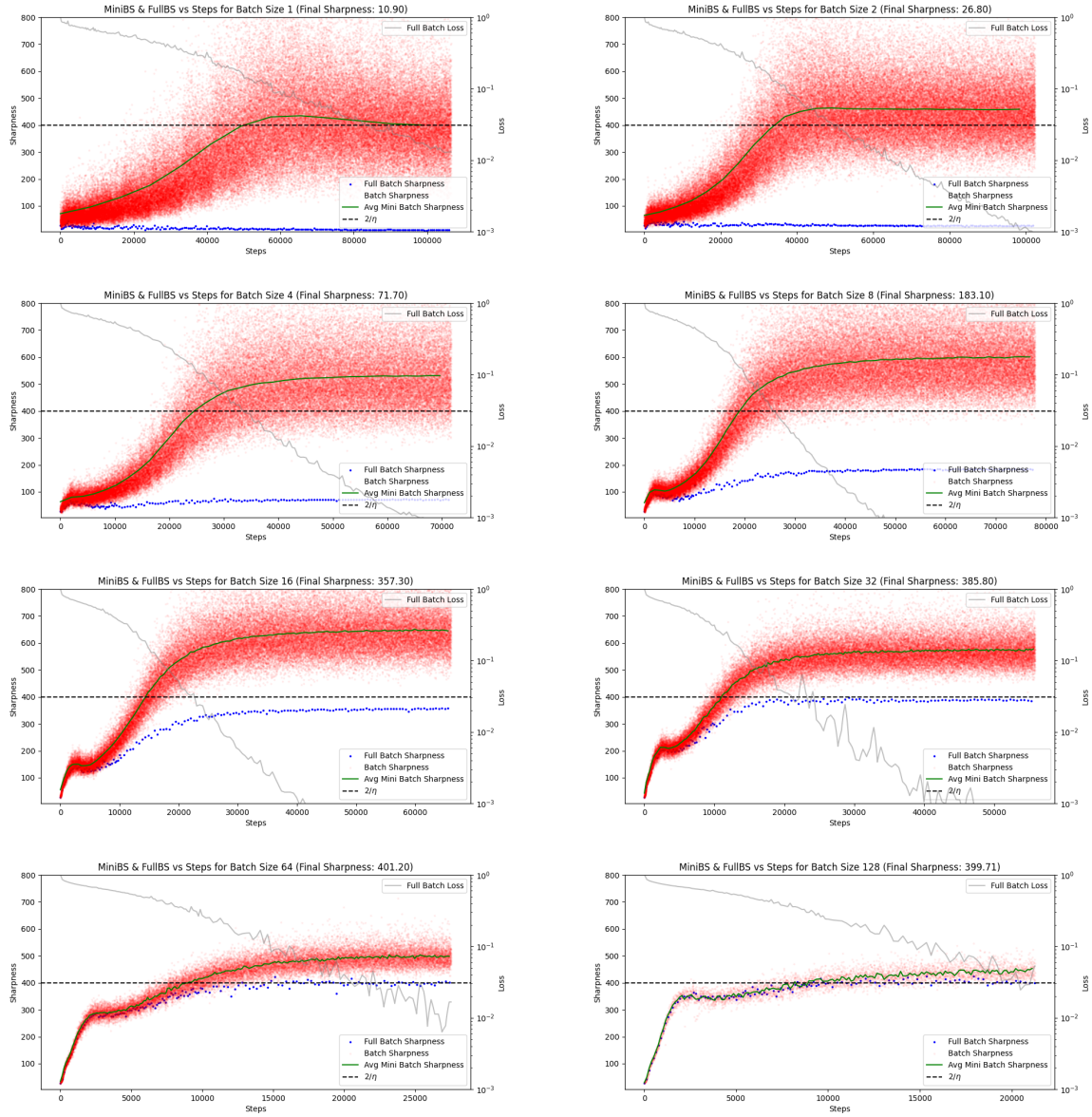


Figure 23. CNN, 4 layers (3 convolutional, 2 fully-connected), LR 0.005, 8k subset of CIFAR-10. Comparison between: the observed highest eigenvalue for the Hessian of the mini-batch loss (red dots), the empirical MINIBS (green line), the FULLBS (blue dots).

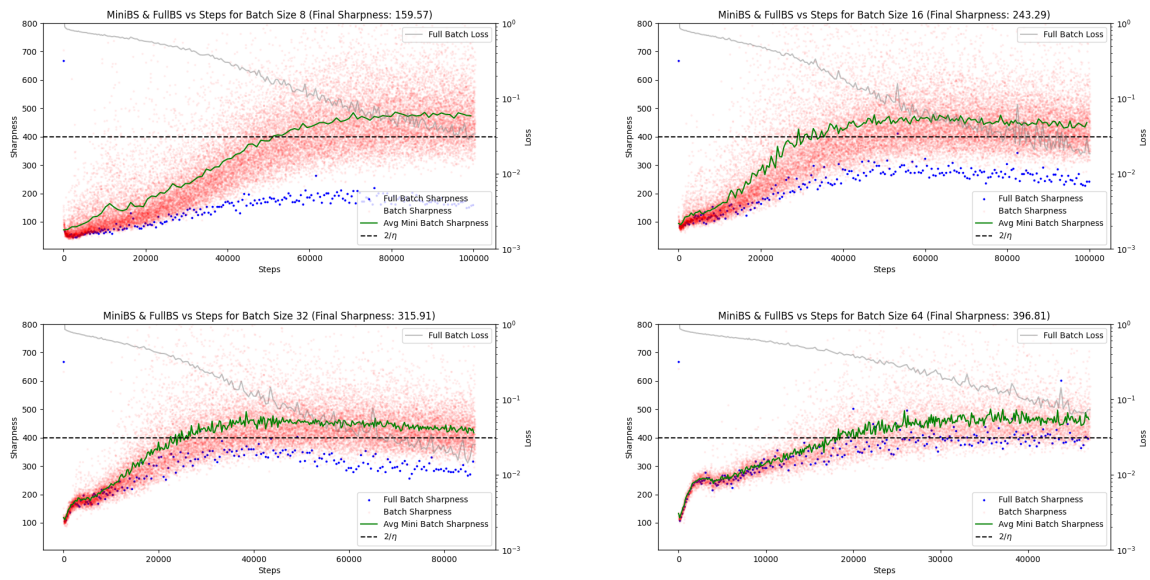


Figure 24. ResNet-10, LR 0.005, 8k subset of CIFAR-10. Comparison between: the observed highest eigenvalue for the Hessian of the mini-batch loss (red dots), the empirical MINIBS (green line), the FULLBS (blue dots).